Journal of Vertebrate Paleontology

ISSN: (Print) (Online) Journal homepage: https://www.tandfonline.com/loi/ujvp20

Comparative braincase morphology of *Trilophosaurus buettneri* and the early evolution of the pan-archosaurian neurocranium

Jacob D. Wilson, Anna Wisniewski, Sterling Nesbitt & Gabriel S. Bever

To cite this article: Jacob D. Wilson, Anna Wisniewski, Sterling Nesbitt & Gabriel S. Bever (2022) Comparative braincase morphology of *Trilophosaurus buettneri* and the early evolution of the pan-archosaurian neurocranium, Journal of Vertebrate Paleontology, 42:1, e2123712, DOI: 10.1080/02724634.2022.2123712

To link to this article: https://doi.org/10.1080/02724634.2022.2123712

Journal of Vertebrate Paleontology e2123712 (21 pages)

DOI: 10.1080/02724634.2022.2123712

ARTICLE

COMPARATIVE BRAINCASE MORPHOLOGY OF *TRILOPHOSAURUS BUETTNERI* AND THE EARLY EVOLUTION OF THE PAN-ARCHOSAURIAN NEUROCRANIUM

JACOB D. WILSON,[1*] ANNA WISNIEWSKI,[2] STERLING NESBITT,[3] and GABRIEL S. BEVER[1*]
[1]Center for Functional Anatomy and Evolution, Johns Hopkins University School of Medicine, 1830 E. Monument St., Baltimore, MD, 21205, U.S.A. jwils183@jhmi.edu; gbever1@jhmi.edu;
[2]Department of the Geophysical Sciences, University of Chicago, 5734 S. Ellis Ave., Chicago, IL, 60637, U.S.A.;
[3]Department of Geosciences, Virginia Tech, 926 W. Campus Dr., Blacksburg, VA, 24061, U.S.A.

ABSTRACT—The relative scarcity of well-preserved fossils from the earliest history of stem lineages often limits our ability to establish robust, broad-based evolutionary patterns. This is certainly the case for the pan-radiation of archosaurs whose earliest stem taxa remain poorly understood relative to the crownward archosauriforms. *Trilophosaurus buettneri* is a North American Triassic stem archosaur that lies near the base of this expansive pan-radiation. We used CT to study the *Trilophosaurus* braincase with the goal of elucidating the early pan-archosaur neurocranium and its evolution. Results clarify several problematic characters including variable fusion of the exoccipital, absence of contralateral exoccipital contact, lack of a semilunar depression, and several others. These novel scorings fail to alter most currently accepted tree topologies, but the results are detailed. These data also include the phylogenetically earliest evidence of neurocranial pneumatization among pan-archosaurs, including a parabasisphenoid cavity that is positionally homologous to the median pharyngeal recess of crown archosaurs. These data are not without their problems, but they do allow us to hypothesize the earliest transformations in what became a much more extensive character system in crown archosaurs. Multiple autapomorphies suggest *Trilophosaurus* was capable of a derived behavioral repertoire, but details remain unclear. For example, *Trilophosaurus* bears a theropod-like elongation of the anterior semicircular canal but lacks the associated expansion of the lateral canal thought to facilitate bipedality in that group. Our data clarify plesiomorphic conditions for later archosaurian transformations while promoting the hypothesis that pan-archosaurs achieved marked structural and behavioral disparity early in their history.

SUPPLEMENTAL DATA—Supplemental materials are available for this article for free at www.tandfonline.com/UJVP

Citation for this article: Wilson, J. D., A. Wisniewski, S. Nesbitt, and G. S. Bever. 2022. Comparative braincase morphology of *Trilophosaurus buettneri* and the early evolution of the pan-archosaurian neurocranium. Journal of Vertebrate Paleontology. DOI: 10.1080/02724634.2022.2123712

INTRODUCTION

The fossil record is a unique source of data that informs two major divisions of evolutionary history – that which is directly ancestral to extant species and the crown clades they define, and that which is unrepresented in the extant biota because it was erased by extinction (Donoghue et al., 1989; Erwin, 2008). In both cases, the empirical contributions of stem-group members tend to skew toward the crown where a larger number of synapomorphies secure the fossils' phylogenetic contribution to the total group. Evolutionary theory predicts that as we sample increasingly deep along any given phylogenetic stem lineage (i.e., towards the theoretical earliest stem member) the number of available, diagnostic synapomorphies will decrease. Fewer derived characters translates to increasing phylogenetic volatility for these fossils with respect to the total group. A by-product of this dynamic is that the early history of both the lineages and the functional complexes that facilitate their eventual evolutionary success is difficult to analyze with empirical rigor.

This basic pattern describes well our understanding of Pan-Archosauria, whose crown is defined by the split between Pan-Crocodylia and Pan-Aves (Pseudosuchia and Avemetatarsalia, respectively, sensu Gauthier, 1986; Benton, 1999). The crown itself and the adjacent, more proximate area of its stem lineage are relatively well studied (Gauthier, 1986; Nesbitt, 2011; Töpfer, 2018). Much less mature is our understanding of the early history of this ~40 my stem lineage (Hedges et al., 2015). Here we find a relatively small number of known taxa, some of which, like the late Permian *Protorosaurus speneri*, might be argued as predictably plesiomorphic (Gottmann-Quesada and Sander, 2009); many, however, are characterized by a highly derived set of morphological features from which we can infer an array of derived behavioral ecologies. The azendohsaurids, tanystropheids, and rhynchosaurs testify convincingly that the high levels of diversity and disparity found in the crown extend well down the stem; still, careful studies of these and other early stem taxa are needed to better understand the extent of their unique paleobiology as well as the evidence they preserve documenting the origin of shared character systems of the crown.

Trilophosaurus buettneri (Case, 1928), is another of these enigmatic, early stem archosaurs. Known primarily from an extensive and near monotypic bonebed in a lower portion of the Dockum Group of Texas (Gregory, 1945), some fragmentary and tooth remains of the taxa are widespread in the lower stratigraphic units of the Chinle Formation and Dockum group across the southwestern U.S.A. (Heckert et al., 2006; Spielmann et al., 2008). The skeletal anatomy of *T. buettneri* was detailed in a

*Corresponding authors.
*Corresponding authors.
Color versions of one or more of the figures in the article can be found online at www.tandfonline.com/ujvp.

Published online 01 Nov 2022

monograph by Gregory (1945), in an unpublished thesis by Parks (1969), in a conference abstract by Merck (1995), in an unpublished PhD dissertation by Merck (1997), and in a collection of works by Spielmann et al. (2005, 2008). These studies concluded *T. buettneri* was a terrestrial herbivore that may have been facultatively bipedal, perhaps even spending time in trees based on ungual recurvature and comparisons with extant reptiles. *Trilophosaurus* was included in a handful of recent phylogenetic analyses but with little agreement regarding its position relative to other key stem archosaurs. For example, there is evidence that *T. buettneri* is part of a moderately sized Triassic radiation called Allokotosauria that includes other Triassic forms such as *Spinosuchus caseanus*, *Teraterpeton hrynewichorum*, and the azendohosaurids (Nesbitt et al., 2015; Ezcurra, 2016; Pritchard and Sues, 2019; Nesbitt et al., 2021). But whether this lineage diverged before both the protorosaurs and tanystropheids (Ezcurra, 2016; Ezcurra and Butler, 2018), between the respective origins of these two groups (Pritchard et al., 2018; Pritchard and Sues, 2019), is nested among the rhynchosaurs (Simões et al., 2018), or is the sister to a *Prolacerta* + Archosauriformes clade (Nesbitt et al., 2015; Pritchard et al., 2015) remains unresolved.

The purpose here is to describe the braincase of *T. buettneri* using μCT (micro-computed tomography), providing novel observations of internal structures and critical annotations of previous observations (all of which were made without the benefit of advanced imaging). These data should form a lasting contribution to the anatomy and evolution of the early pan-archosaur braincase – a character complex viewed as relatively conservative among cranial modules (Gow, 1975; Parrish, 1993; Gower and Sennikov, 1996).

Institutional Abbreviations—**AMNH**, American Museum of Natural History, New York City, NY, U.S.A.; **BPI**, Evolutionary Studies Institute (formerly Bernard Price Institute for Palaeontological Research), University of the Witwatersrand, Johannesburg, South Africa; **FMNH**, Field Museum of Natural History, Chicago, IL, U.S.A.; **PIMUZ**, Palaeontological Institute und Museum Universität Zürich, Zürich, Switzerland; **SAM**, Iziko South African Museum, Cape Town, South Africa; **TM**, Transvaal Museum, Pretoria, South Africa; **TMM**, Texas Memorial Museum, Austin, TX, U.S.A.; **UCMP**, University of California Museum of Comparative Zoology, Berkeley, CA, U.S.A.; **UMZC**, University Museum of Zoology, Cambridge, UK.

MATERIALS AND METHODS

Our study focuses on the neurocranial morphology of TMM 31025-244, an articulated and largely undistorted braincase (lacking dermal roofing elements) collected by G. Meade at Otis Chalk Quarry 1 (=*Trilophosaurus* quarry, TMM 31025) in the lower portion of the Triassic Dockum Group (Late Carnian; Dunay and Fisher, 1979, Hunt and Lucas, 1991), Howard County, Texas. The specimen was collected and cataloged as an isolated discovery, which means its historical assignment as *T. buettneri* (hereafter referred to simply as *Trilophosaurus*) must be carefully and critically considered. That assignment draws heavily from the conclusion that *Trilophosaurus* is the dominant taxon in Quarry 1. This representation includes several partially articulated specimens, a minimum of 45 individuals, and 1001 of 1144 cataloged specimens (87.5%, Elder, 1987; TMM database). Not all these identifications can or should be considered independent, so there is clear danger of circular reasoning when considering these numbers as taxonomic support for any given specimen. Still, many of these cranial and post-cranial elements do exhibit well-established autapomorphies, and there is no evidence the site is taxonomically diverse and more than one *Trilophosaurus* species is present. TMM 31025-244 also closely resembles the other six braincases currently assigned to *Trilophosaurus* from the same locality, although phenetic resemblance may be driven by plesiomorphic features that are of limited taxonomic relevance within a phylogenetic system (Patterson and Rosen, 1977; Bever, 2005; Nesbitt and Stocker, 2008; Bell et al., 2010). But as we detail here, TMM 31025-244 has autapomorphic features that solidify its identity as *Trilophosaurus*. The information content of these features is subject to testing by additional sampling in this part of the tree, but such is the case for all putative apomorphies.

The decision to build our description around TMM 31025-244 reflects the general quality of its preservation as well as the clarity of its associated μCT images. We do make comparisons with two other braincases referred to *Trilophosaurus* (TMM 31025-140 and TMM 31100-443; Fig. 1). We have surface scans and μCT data for both specimens and use them to note variation where observed. A comprehensive survey of braincase variation in *Trilophosaurus* – one involving all known specimens – is planned but will require considerable additional physical and digital preparation. We consider it worthwhile to publish available observations now, especially considering the recent appearance of contributions that shed much-needed light on the braincase of other early stem archosaurs (e.g., Sobral and Müller, 2019; Miedema et al., 2020).

The three examined *Trilophosaurus* specimens are approximately the same size based on the height of the occipital condyle; although, this metric is not a wholly reliable ontogenetic indicator (Hone et al., 2016). Based on a more general assessment of size, morphology, and sutural closure (following Griffin et al., 2021), we conclude that all three specimens represent the later stages of skeletal maturity, although some age disparity is likely using these methods. This disparity is neither unique to our sample nor is it insignificant given that peri- and endochondral ossification of the neurocranium continues during even the last stages of post-natal ontogeny with resultant complications for character delineation and assessment (see Discussion).

Previous, externally based descriptions of the *Trilophosaurus* braincase were provided by Gregory (1945) and Parks (1969), with the observations of Parks being reprinted as part of Spielmann et al. (2008). *Trilophosaurus* was also included in several phylogenetic analyses that include braincase characters (e.g., Nesbitt et al., 2015; Ezcurra, 2016; Simões et al., 2018; Pritchard et al., 2018). These observations appear to be largely based on TMM 31025-140 and TMM 31100-443, although Parks (1969) included TMM 31025-244 in his reconstruction and description of the supraoccipital, basisphenoid, and prootic. As the first μCT-based braincase description in this taxon, it is also the most anatomically comprehensive.

Throughout the description, we make comparisons with a small, but phylogenetically informed selection of species, including the stem reptile *Youngina capensis* (AMNH 5561, FMNH UC 1528, and TM 3603, Evans, 1987; FMNH UC 1528 and AMNH 5561, Gardner et al., 2010) and four stem archosaurs: *Macrocnemus bassanii* (PIMUZ T 2477, Miedema et al., 2020), *Mesosuchus browni* (SAM-PK 6536; Dilkes, 1998, Sobral and Müller, 2019), *Prolacerta broomi* (BPI/1/2675, UCMP 37151, and UMZC 2003.40, Evans, 1986), and *Euparkeria capensis* (UMZC T.692, Gower and Weber, 1998; UMZC T.692, SAM-PK-5867, SAM-PK-6047A, and SAM-PK-7696, Sobral et al., 2016). Most comparative observations included here are drawn from the studies listed with each taxon; we do not cite these in each instance for the sake of brevity. In cases where the observations are derived uniquely from our own examination of specimens, CT data, or published figures, those details are cited explicitly. A broadened set of comparisons is the basis of our Discussion and is derived in part from the rerunning of several recent phylogenetic analyses with alternative scorings for *Trilophosaurus*. The re-analyzed matrices are those of Pritchard et al. (2018), Pritchard and Sues (2019), Ezcurra (2016), Scheyer et al. (2020), and Stocker et al.

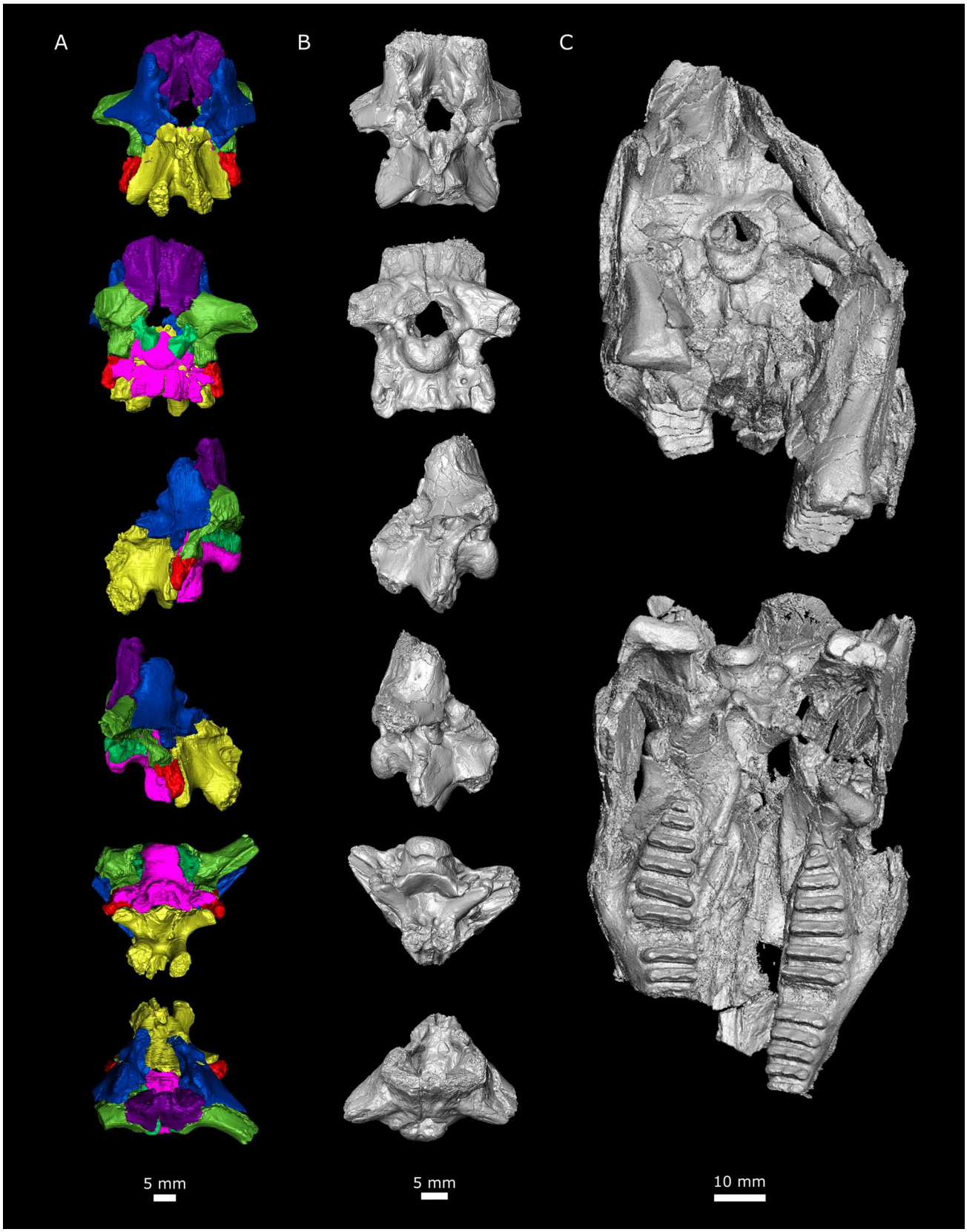

FIGURE 1. Specimens of *Trilophosaurus buettneri* described herein. **A** and **B**, TMM 31025-244 and TMM 31100-443, respectively, in (descending order) anterior, posterior, left lateral, right lateral, ventral, and dorsal views; **C**, TMM 31025-140 in (descending order) posterior and ventral views.

(2016). For the Stocker et al. (2016) matrix, we added a new character – absence (0)/presence (1) of an elongated anterior semicircular canal. Our re-analyses used the parsimony search parameters of the original authors (analysis 3 from Ezcurra, 2016 and analysis 1 from Scheyer et al., 2020) and considered the impacts of the alternative scorings first collectively then individually if tree topology was altered. See the readme file in the supplemental information for step-by-step information on the phylogenetic analysis.

TMM 31025-244 was scanned in 2008 at the High-Resolution X-Ray Computed Tomography Facility at The University of Texas at Austin (UTCT) using a voltage of 210 kV and an amperage of 0.11 mA. Scanning produced 225 coronal slices with voxel dimensions of 0.04 mm (X), 0.04 mm (Y), and 0.05 mm (Z). TMM 31025-140 and TMM 31100-443 were scanned in 2019 at the Duke University Shared Materials Instrumentation Facility (SMIF) using a voltage of 220 and 225 kv and amperage of 254 and 108 mA, respectively. Both scans produced cubic voxels of 0.06 mm (140) and 0.2 mm (443). We used Amira 6.3.0 to digitally segment the individual neurocranial bones of TMM 31025-244 and to construct an endocast of the inner ear. Segmentation was attempted for both ears, but damage permitted a complete endocast for the right side only. All three specimens were physically prepared prior to CT scanning. Micro CT data in the form of TIF image stacks are available for all specimens under Morphosource project ID: 000440518 (https://www.morphosource.org/projects/000440518).

The taxonomic history of *Trilophosaurus buettneri* is worth noting here. The holotype of *Trilophosaurus buettneri* consists of a tooth-bearing fragment bearing some complete teeth (UMMP 2339; Case, 1928) from the Tecovas Formation of Crosby County, Texas. In the late 1930s, hundreds of bones including partial skeletons were found at a single locality, Otis Chalk Quarry 1 (TMM 31025) from the Colorado City Member of the Cooper Canyon Formation of the Dockum Group (Stocker, 2013), Howard County, Texas. These remains were referred to *Trilophosaurus buettneri* by Gregory (1945) and this assignment has been followed by many authors (e.g., Parks, 1969; Heckert et al., 2006; Spielmann et al., 2008). Furthermore, the specimens from TMM 31025 served as a proxy 'type' (sensu Parker, 2013) for *Trilophosaurus buettneri* by comparing the taxon with other reptiles and for scoring the taxon into phylogenetic matrices (e.g., Dilkes, 1998; Nesbitt et al., 2015), particularly TMM 31025-140, a nearly complete skeleton detailed by Gregory (1945). We follow the referral of the *Trilophosaurus* remains from TMM 31025 to *Trilophosaurus buettneri.* Thus, all of the braincases that share apomorphies with TMM 31025-140, a specimen with teeth referable to the holotype of *Trilophosaurus buettneri* and a complete braincase, are considered assignable to *Trilophosaurus buettneri*. There are now several *Trilophosaurus* species (e.g., *T. buettneri*, *T. jacobsi*, *T. dornorum*, and *T. phasmalophos*) based largely on dental remains, so characters found in the braincase of the referred specimens of *Trilophosaurus buettneri* from TMM 31025 may pertain to these other *Trilophosaurus* species also and are here discussed as *Trilophosaurus* apomorphies (see Discussion).

RESULTS

Description

General—The neurocrania of TMM 31025-244 and TMM 31100-443 are fully articulated, largely complete, and without significant distortion. Preserved elements include the paired exoccipitals, opisthotics, and prootics, and the midline basioccipital, supraoccipital, and parabasisphenoid (Fig. 2). The braincase of TMM 31025-140 is less complete and shows significant anterior distortion. We observed no basisphenoid-parasphenoid suture, and thus refer to the fused structure as the 'parabasisphenoid.' Dermal roofing elements (frontals, parietals) are known for *Trilophosaurus* (Gregory, 1945; Parks, 1969; Elder, 1987; Spielmann et al., 2008) but are not associated with TMM 31025-244 nor described here. The stapes is lost in TMM 31025-244 and TMM 31100-443 but partially preserved on the right side in TMM 31025-140. There is no evidence of a laterosphenoid; this includes the absence of any obvious sutural ridges on the prootic or parietal. The laterosphenoid is historically considered a more crown-ward feature diagnosing Archosauriformes (Clark et al., 1993), although it was reported in the non-archosauriform *Azendohsaurus madagaskarenesis* (Flynn et al., 2010) and even among some stem turtles (Bhullar and Bever, 2009; Bever et al., 2015). There is a paired ossification in close association with the basituberа (Fig. 2; sbt). It was referred to as the "'X' bone" by Parks (1969) and shares connectivity with a bone often referred to as 'Element X' in the squamate literature. It was suggested by Parks (1969) that the bone represents a short length of ossified tendon from m. longissimus capitis—a hypothesis we accept with revision (see below). We advocate referring to this ossification as the os sesamoideum basituberum (see Discussion).

The composite shape of the neurocranium differs from that of most early diverging pan-archosaurs in being anteroposteriorly short and dorsoventrally deep (Fig. 2C, D). These exaggerated dimensions are reflected in the *Trilophosaurus* skull as a whole (Gregory, 1945:fig. 4), and possibly reflect the reorganization of the skull to withstand high occlusal forces, alongside a peaked palate and vaulted parietals (Merck, 1997). Several neurocranial elements contain internal cavities; some of these spaces open externally and occupy positions homologous to those of known pneumatic recesses of crown archosaurs (see Discussion). Only the cultriform process and lateral ends of both paroccipital processes are obviously missing from TMM 31025-244. Overall, distortion is worse on the left side where it results in a large gap between the supraoccipital and left prootic; the right side is largely undamaged.

Exoccipital—The exoccipitals are short, strut-like elements oriented along an oblique ventromedial-to-dorsolateral plane

→FIGURE 2. *Trilophosaurus buettneri* TMM 31025-244 braincase in **A**, anterior view; **B**, posterior view; **C**, left lateral view; **D**, right lateral view; **E**, ventral view; **F**, dorsal view. **Abbreviations**: **ap.bo**, anterior plate of the basioccipital; **aip.pr**, anterior inferior process of the prootic; **bp.bs**, basipterygoid processes of the parabasisphenoid; **bt.bs**, basitubera of the parabasisphenoid; **cc.bs**, carotid canals of the parabasisphenoid; **cf.bs**, cultriform process of the parabasisphenoid; **ci.op**, crista interfenestralis of the opisthotic; **cp.bs**, cultriform process of the parabasisphenoid; **cp.pr**, crista prootica; **d.V**, depression of the trigeminal ganglion; **ds.bs**, dorsum sellae of the parabasisphenoid; **fic.bs**, possible foramen into open space in parabasisphenoid; **fm**, foramen magnum; **fr**, fracture; **fv**, fenestra vestibuli; **ld.so**, lateral depression on the supraoccipital; **mc.so**, midline concavity of the supraoccipital; **mf**, metotic fissure; **mpr**, median pharyngeal recess; **mr.bo**, midline ridge of the basioccipital; **mr.bs**, midline ridge of the parabasisphenoid; **mt.so**, midline trough of the supraoccipital; **oc.bo**, occipital condyle of the basioccipital; **p.asc**, prominence of the anterior semicircular canal; **pf.bs**, pituitary fossa of the parabasisphenoid; **ppr.op**, paroccipital process of the opisthotic; **sbt**, os sesamoideum basituberum (Element X); **sr**, stapedial recess; **t.bo**, lateral tabs on the basioccipital; **up.so**, u-shaped process of the supraoccipital; **V**, foramen for CN V; **vcm**, notch for the medial cerebral vein; **VI**, notch from CN VI; **VII**, foramen for CN VII; **vp.pr**, ventral process of the prootic; **vr.op**, ventral ramus of the opisthotic; **XII**, foramina for CN XII.

(Figs. 2B, S1). Each one contacts the opisthotic dorsally and basioccipital ventrally. In TMM 31025-244, the exoccipitals remain unfused to these neighboring elements, whereas in TMM 31025-140 and TMM 31100-443 the sutures are closed. The exoccipitals of *Youngina* and *Prolacerta* are variably fused to the basioccipital; when unfused, they also contribute to the

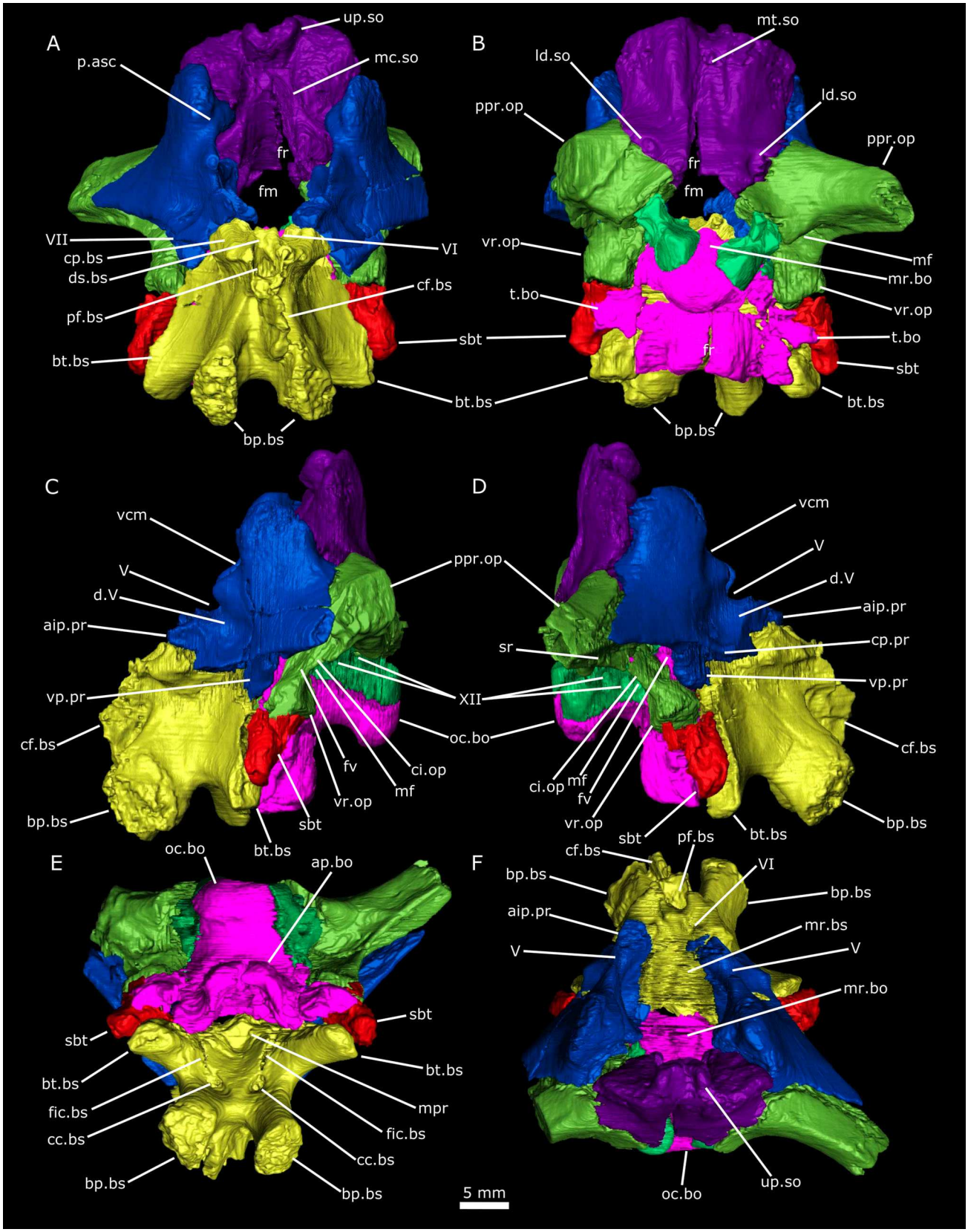

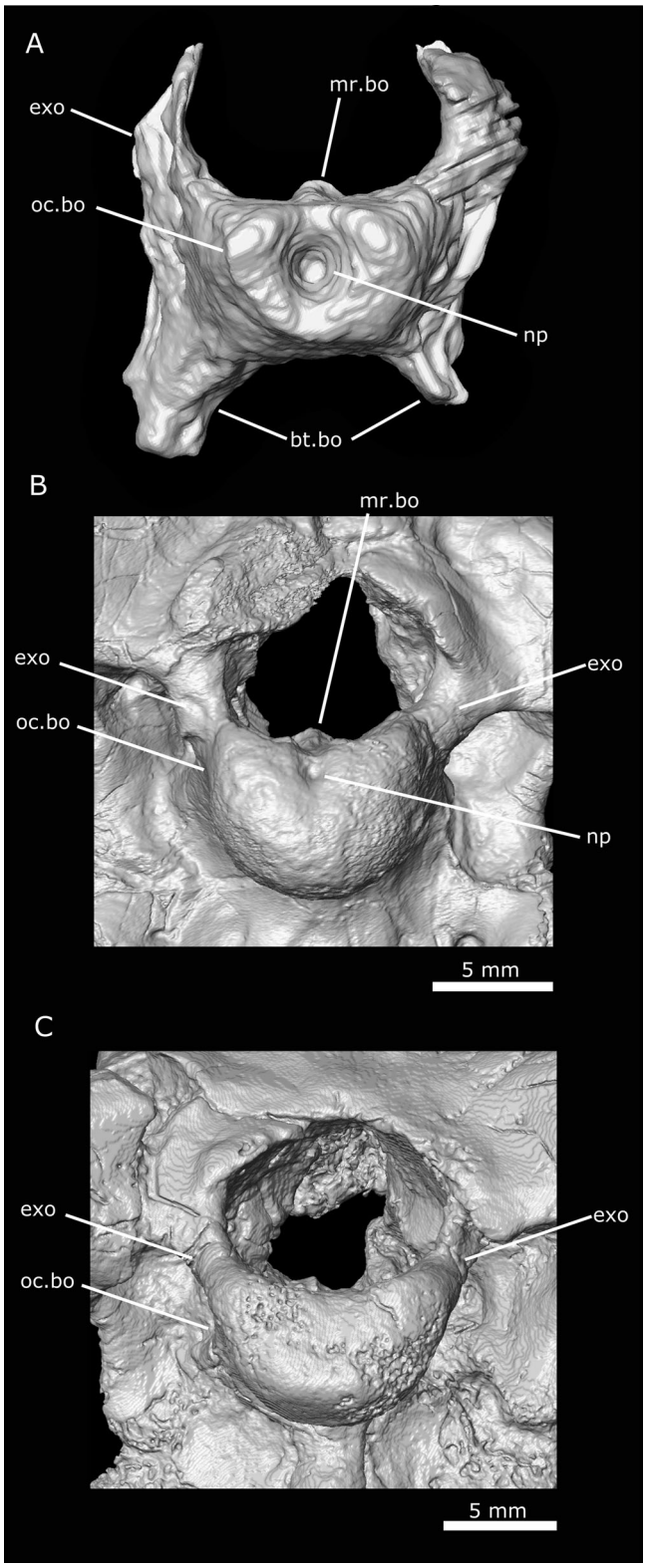

FIGURE 3. Details of occipital condyles in *Trilophosaurus buettneri* and *Youngina capensis*. **A**, *Youngina capensis* specimen AMNH 5561 posterior view of basioccipital; **B**, *Trilophosaurus buettneri* specimen TMM 31100-443 posterior view of occipital condyle; **C**, *Trilophosaurus buettneri* specimen TMM 31025-140 posterior view of occipital condyle. **Abbreviations**: **bt.bo**, basitubera of basioccipital; **exo**, exoccipital; **mr.bo**, medial ridge of basioccipital; **np**, notochordal pit; **oc.bo**, occipital condyle of basioccipital.

occipital condyle and lack a midline contact (as in *Macrocnemus*, *Mesosuchus*, and *Euparkeria*). The quadrangular, slightly hourglass, shape of the exoccipital in posterior view is driven by terminal expansions that buttress the element against the basioccipital and opisthotic, and by the concave, medial margin that circumscribes the ventrolateral circumference of the foramen magnum (Fig. 2B, 3B, C).

In TMM 31025-244, the contralateral exoccipitals stop well short of a ventral, midline contact, permitting a basioccipital contribution to the foramen magnum and restricting the exoccipitals to the dorsolateral corners of the occipital condyle (Fig. 2B). The paired exoccipitals form only a small part of the foramen magnum's dorsolateral margin, which is dominated by the supraoccipital but with a narrow contribution from both opisthotics (Fig. 2B). This morphology is consistent with that of *Youngina* and many pan-archosaurs (including *Macrocnemus*, *Mesosuchus*, and *Euparkeria*). In *Prolacerta* specimen UC 37151, the exoccipitals do not contact dorsally, whereas in specimen BPI 2675 the exoccipitals reach the dorsal midline of the foramen. The lateral margin of the exoccipital is continuous with the ventral margin of the paroccipital process. In this sense, the exoccipitals contribute to the base of the process (Fig. 2B) but do not constitute its majority as ascribed by Parks (1969). Parks also described an exoccipital-supraoccipital contact that we could not observe with CT data. A pair of hypoglossal canals (CN XII) penetrate both exoccipitals, with the external foramen of the anterior canal located slightly ventral to that of the posterior canal (Figs. 2C–D, 4A: XII). The configuration represents the plesiomorphic condition for Pan-Archosauria (Nesbitt, 2011) also retained in *Prolacerta* and *Euparkeria*. *Youngina* shows a variable number of hypoglossal foramina (Evans, 1987), and the foramina are arranged more vertically in *Mesosuchus*. Anteriorly, the exoccipital forms the posterior wall of an undivided metotic fissure (conveying CNs IX–XI and the lateral head vein [Gower and Weber, 1998]; Fig. 2C, D: mf).

Basioccipital—The basioccipital is slightly taller than long. Its anteroposterior length is roughly equal to the more anterior parabasisphenoid with which it forms a basically transverse suture (Figs. 2C, D, F, S2). This morphology is similar to *Euparkeria*, but contrasts with *Youngina*, *Macrocnemus*, *Mesosuchus*, and *Prolacerta* wherein the parabasisphenoid is dominant in its anteroposterior contribution to the floor of the braincase. The suture with the parabasisphenoid, like that of *Mesosuchus* and *Euparkeria*, is tightly formed and transverse, contrasting with the more open, overlapping suture of *Youngina*, *Macrocnemus*, and *Prolacerta*. Lateral contact with the opisthotic is broad, whereas the anterolateral suture with the prootic is more restricted. The posterior end of the basioccipital receives the exoccipitals dorsolaterally (Fig. 2B).

The articular surface of the occipital condyle of TMM 31100-443 bears a distinct but small notochordal pit (Fig. 3B; np). Both TMM 31025-244 and TMM 31025-140 have shallow depressions on the posterior surface of the condyle and are thus similar to the condyle of *Macrocnemus bassani* (Fig. 3C). *Youngina* has a notochordal pit (Fig. 3A), whereas *Prolacerta* and *Euparkeria* have smooth, convex condyles. The condyle of *Mesosuchus* is scored as lacking a notochordal pit or bearing a small one by Scheyer et al. (2020) and Ezcurra (2016), although we find the posterior surface is too damaged to make this observation (Sobral and Müller, 2019; our observations of fig. 3). The occipital condyle has a distinct ventral lip that in lateral view exaggerates the neck-like connection between the condyle and the main body of the basioccipital, in contrast to the condition in *Youngina*, *Macrocnemus*, *Mesosuchus*, *Prolacerta*, or *Euparkeria*.

The ventral surface of the basioccipital is broadly concave—a shape exaggerated posteriorly by the occipital condyle and anteriorly by a vertical plate that extends well below the ventral

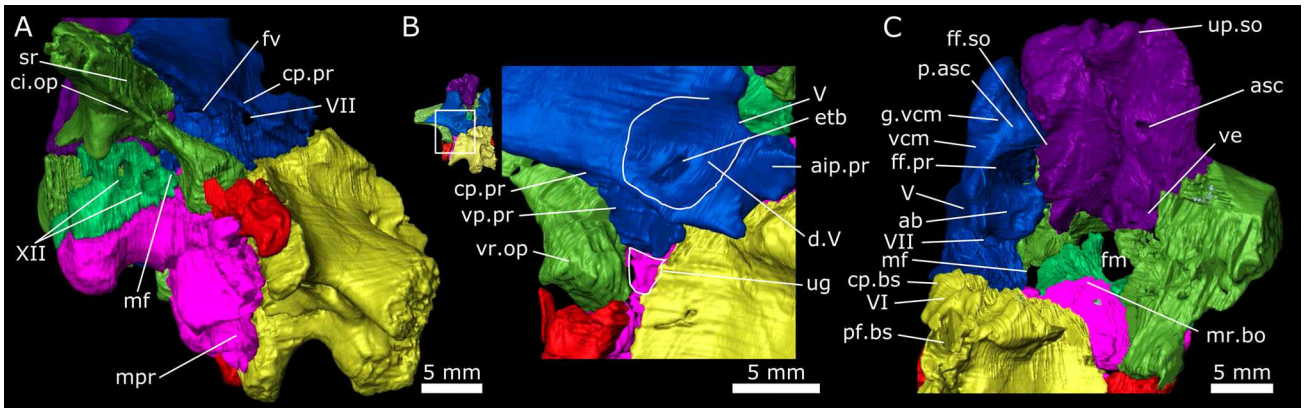

FIGURE 4. *Trilophosaurus buettneri* TMM 31025-244 braincase in **A**, right ventrolateral view; **B**, right anterolateral view, showing depression for trigeminal ganglion and unossified opening into lagenar recess; **C**, left anterodorsal view with left prootic removed. **Abbreviations**: **ab**, ampullary bulla; **aip.pr**, anterior inferior process of the prootic; **asc**, anterior semicircular canal; **ci.op**, crista interfenestralis of the opisthotic; **cp.bs**, clinoid process of the parabasisphenoid; **cp.pr**, crista prootica; **d.V**, depression of the trigeminal ganglion; **etb**, extreme thinning of bone; **ff.pr**, floccular fossa in prootic; **ff.so**, floccular fossa in supraoccipital; **fm**, foramen magnum; **fv**, fenestra vestibuli; **g.vcm**, groove for the medial cerebral vein; **mf**, metotic fissure; **mpr**, median pharyngeal recess; **mr.bo**, median ridge of the basioccipital; **p.asc**, prominence of the anterior semicircular canal; **pf.bs**, pituitary fossa of the parabasisphenoid; **sr**, stapedial recess; **ug**, unossified gap; **up.so**, u-shaped process of the supraoccipital; **V**, foramen for CN V; **vcm**, notch for the medial cerebral vein; **ve**, vestibule of the inner ear; **VI**, groove for CN VI; **VII**, foramen for CN VII; **vp.pr**, ventral process of the prootic; **vr.op**, ventral ramus of the opisthotic; **XII**, foramina for CN XII.

surface of the occipital condyle (Fig. 2C–E). Running down the posterior midline of the plate in TMM 31100-443 and TMM 31025-140 is a ridge that is not preserved in TMM 31025-244 (Fig. 5A: r.bo). The lateral margins of this plate include small tabs that contribute to the posterior surface of the basituberal processes (Figs. 2B, 5A: t.bo). These tabs also contact the os sesamoideum basituberum but are not derived from it (clear only in TMM 31100-443). In TMM 31100-443, the tab on the basioccipital forms the posterior wall of a short, blind, unossified recess that is walled anteriorly by the parabasisphenoid, laterally by the os sesamoideum basituberum, and medially by the basioccipital. This is the poorly named 'pseudolagenar recess,' a space hypothesized to be cartilage-filled in life and presenting no apparent connection to the inner ear (Gower and Sennikov, 1996). This unossified fossa is distinct from the unossified gap described below that would have contained the lagena. At the base of the tab on the right side of TMM 31100-443 is a foramen that may be pneumatic in origin (Fig. 5A, see description below). The inferior margin of the plate does not quite reach the lateral end of the parabasisphenoid portion of the basitubera (Fig. 2C, D). As part of the basitubera, the plate represents a robust contact surface for the prevertebral muscles, which attach to the posterior face of the basitubera in crown archosaurs such as *Caiman crocodilus* and *Struthio camelus* (m. rectus capitis anterior and m. longissimus capitis; Gregory, 1945; Tsuihiji, 2007).

A posterior view of the plate reveals a slightly oblique, median cleft whose asymmetry suggests a break (Fig. 2B: fr). The plate's ventral margin is straight in TMM 31025-244 and TMM 31100-443 but emarginated in TMM 31025-140. Anteriorly, the plate is deeply concave, forming the thickened posterior wall of a large, circular, ventral recess (Fig. 4A, 6A, B: mpr). This recess extends anteriorly onto the parabasisphenoid where it is delimited in part by the bases of the basipterygoid processes. A shallower recess is present in *Youngina* (Fig. 6C), *Mesosuchus* (Fig. 6D), and *Euparkeria* but is lacking in *Prolacerta*. The condition in *Macrocnemus* is unclear, although no ventral recess is described. The closely related *Tanystropheus hydroides* (Spiekman et al., 2021) has a ventral recess that, with the recesses in *Mesosuchus* and other more crownward stem archosaurs, shares positional, primary homology with the median pharyngeal recess of crown Archosauria (see Discussion).

The basioccipital of *Trilophosaurus* has a broad anterior plate that is lacking in our comparative sample (see Discussion). *Youngina*, *Macrocnemus*, *Mesosuchus*, and *Euparkeria* have wing-like structures that contribute to the basitubera. *Prolacerta* exhibits a ridge-like connection of the paired basitubera that is sometimes referred to as the intertuberal plate (see Spiekman et al., 2021). In contrast to the anterior plate in *Trilophosaurus*, the intertuberal plate is typically a horizontal feature and is part of the parabasisphenoid. This feature is lacking in *Trilophosaurus*, *Youngina*, *Macrocnemus*, *Mesosuchus*, and *Euparkeria*.

Considered in isolation, the posterodorsal surface of the basioccipital is convex, with the oblique exoccipital facets sloping ventrally and laterally from a high median ridge. With the exoccipitals, the basioccipital forms the concave ventral margin of the foramen magnum and the posterior floor of the hindbrain. A median dorsal ridge representing the medial sulcus of the hindbrain (Evans, 1986) is present across the length of the basioccipital and continues onto the parabasisphenoid (perhaps not in TMM 31025-140) (Figs. 2F, 3B: mr.bo, mr.bs). The ridge is present in *Youngina* (Fig. 3A), *Mesosuchus*, *Prolacerta*, and *Euparkeria* but not *Macrocnemus*.

Parabasisphenoid—The parabasisphenoid dominates the anterior end of the neurocranium, contacting the prootics dorsolaterally, basioccipital posteriorly, and os sesamoideum basituberum posterolaterally (Figs. 2C, D, S3). The ventral ramus of the opisthotic approaches but does not contact the parabasisphenoid in TMM 31025-244; a narrow contact is present in TMM 31025-140 and TMM 31100-443, similar to the condition in *Euparkeria*. *Youngina*, *Mesosuchus*, and *Prolacerta* exhibit a parabasisphenoid-opisthotic contact whereas *Macrocnemus* does not. There is a small gap between the posterolateral corner of the parabasisphenoid, ventral ramus of the opisthotic, and ventral projection of the prootic (Figs. 4B, 5B: ug). In TMM 31025-244 and TMM 31100-443 (cannot confirm in TMM 31025-140), a channel trends medial to the gap, continuing dorsally to the ventral margin of the foramen vestibuli; collectively, these spaces may represent the lagenar recess (Nesbitt, 2011). In *Mesosuchus*, the lagena was contained in a depression on the dorsal surface of the basioccipital. In *Prolacerta* and *Euparkeria*, the lagena was contained in a gap located directly ventral to the ventral surface of the descending ramus of the opisthotic (Sobral

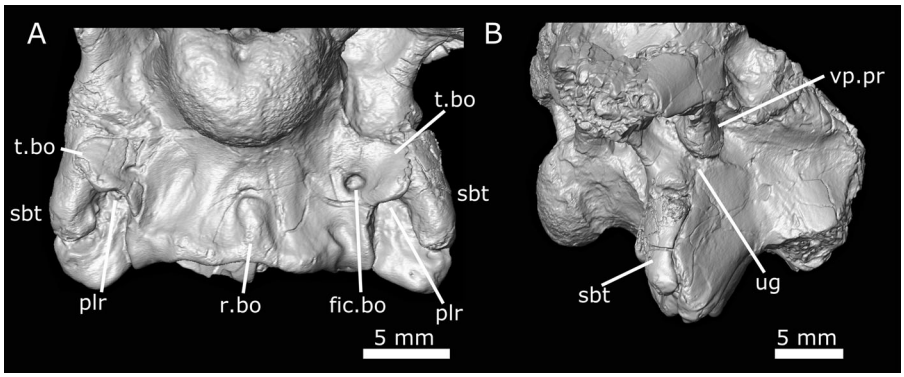

FIGURE 5. *Trilophosaurus buettneri* details of posterior and lateral braincase. TMM 31100-443 in **A**, posterior view; **B**, lateral view. **Abbreviations**: **fic.bo**, possible foramen into open space in the basioccipital; **plr**, pseudolagenar recess; **r.bo**, ridge on the posterior face of the basioccipital; **sbt**, os sesamoideum basituberum (Element X); **t.bo**, lateral tabs on the basioccipital; **ug**, unossified gap; **vp.pr**, ventral process of the prootic.

et al., 2016). The lateral wall of the braincase in *Youngina* and *Macrocnemus* is marked by a large unossified area roughly delimited by the prootic, parabasisphenoid, and opisthotic. The lagenar recess in *Youngina* likely was continuous with the large unossified area and descended along the ventral ramus of the opisthotic (Gardner et al., 2010).

The relatively short length and tall height of the parabasisphenoid is driven by the paired basituberal and basipterygoid processes (all but the base of the cultriform process is missing). The finger-like basitubera project ventrolaterally and slightly posteriorly, closely resembling those of *Mesosuchus*, *Macrocnemus*, and *Euparkeria* but contrasting with the more ridge-like basitubera of *Youngina* and *Prolacerta* (Fig. 2C, D). *Trilophosaurus* and *Macrocnemus* lack the semilunar depression marking the posterolateral aspect of the basitubera of many early diverging pan-archosaurs including *Mesosuchus*, *Prolacerta*, and *Euparkeria*. The basitubera extend further laterally than the larger basipterygoid processes whose anteroventral orientation is shared with *Mesosuchus* and *Euparkeria* (perhaps indicating a derived function in transmitting occlusal forces from the tooth row to the parietals) and contrasts with the more horizontal processes of *Youngina* and *Prolacerta* (*Macrocnemus* is intermediate). The lateral face of the parabasisphenoid lacks the parasphenoid crest that floors the vidian canal in *Youngina* and *Prolacerta* and is scored as present in *Mesosuchus* and *Euparkeria* (Ezcurra, 2016; Pritchard et al., 2018; Pritchard and Sues, 2019). This crest also appears absent in *Macrocnemus*. The parabasisphenoid houses most of the ventral recess described above, forming its anterior and lateral walls. The circular apex of the recess lies just in front of the basioccipital-parabasisphenoid suture (Figs. 2E, 4A, 6A, B: mpr). The recess lacks internal bony divisions, including the transverse intertuberal plate (see above).

As in *Youngina*, *Mesosuchus*, *Prolacerta*, and *Euparkeria* (unclear for *Macrocnemus*), the carotid canals are large and penetrate the ventral surface of parabasisphenoid just posterior to the basipterygoid processes and on either side of the sagittal midline before converging in the base of the dorsum sellae (Figs. 2E, 6A: cc.bs). The lateral walls of the pituitary fossa thicken dorsally forming a plate-like upper surface that would have supported the cartilaginous pila antotica (Fig. 7A: ds.bs; Bellairs and Kamal, 1981). When viewed anteriorly and considered with the basiptergyoid processes, these structures give the parabasisphenoid a markedly X-like shape (Fig. 2A). The base of the cultriform process is retained as a vertical plate extending from the sella turcica between the basipterygoid processes (Figs. 2A, F, 7A: cf.bs). In TMM 31025-244, it is slightly distorted to the left but would have supported the midline ethmoid cartilage (Bellairs and Kamal, 1981).

A narrow crista sellaris is flanked by a pair of grooves representing the path of the abducens nerve (CN VI; Figs. 2A, 7A: VI). These grooves trend just medial to the articulation with the prootics as they do in *Youngina* and in contrast to *Prolacerta* where they traverse the prootic facets and in *Euparkeria* where they pierce the dorsum sellae. No abducens path is described for *Macrocnemus* or *Mesosuchus*, nor could we find the groove in the *Mesosuchus* CT data. The dorsum sellae is high and narrow and sits between the prootic facets. The parabasisphenoid-prootic contact does not converge on the midline as starkly as found in *Prolacerta*, *Mesosuchus*, or *Euparkeria*. Nor does it show the parallel orientation of *Youngina*—*Trilophosaurus* and *Macrocnemus* show an intermediate condition. Posterior to the dorsum sellae, the parabasisphenoid is dorsally concave with the weak median ridge described above (Fig. 2F, 7A: mr.bs).

Prootic—The paired prootics are slightly taller than long (Figs. 2C–D, S4) and form contacts with the parabasisphenoid ventrally and the supraoccipital and opisthotics posteriorly. Their overall triangular shape is driven by a posterolaterally directed lamina that forms a broad contact with the opisthotic and contributes to the anterior face of the paroccipital process (Fig. 2D). The same contact occurs in *Mesosuchus*, *Prolacerta*, and *Euparkeria* but not *Youngina* or *Macrocnemus*. This is a feature of Pan-Archosauria that transforms to a narrow contact within pan-crocodylians (Nesbitt, 2011).

The anterodorsal edge of the prootic is marked by a pair of notches (Fig. 2C, D) reflecting the partitioning of the middle cerebral vein from the trunk of the trigeminal nerve (O'Donoghue, 1920; Oelrich, 1956; Porter and Witmer, 2015) —a bony separation that is absent in *Youngina*, *Macrocnemus*, *Mesosuchus*, *Prolacerta*, and *Euparkeria*. The larger and more anteroventrally placed prootic incisure (CN V) is framed ventrally by the anterior inferior process of the prootic as in *Macrocnemus*, *Mesosuchus*, *Prolacerta*, and *Euparkeria* but not *Youngina*. The process bears a small ridge that is described as a continuation of the crista prootica in *Macrocnemus* and is also present in *Mesosuchus*, *Prolacerta*, and *Euparkeria*. A depression for the trigeminal ganglion (Oelrich, 1956) marks the external prootic surface just below the prootic incisure (Fig. 4B: d.V). Its thin wall bears an opening into the cranial cavity that is absent in TMM 31100-443 and likely represents a preservational artifact (Fig. 4B: etb).

The crista prootica extends from ventral to the anterior inferior process of the prootic to the base of the paroccipital process (Figs. 2D, 7B: cp.pr). It is present in *Macrocnemus*, *Mesosuchus*, *Prolacerta*, and *Euparkeria*, but is either limited (only over the foramen for CN VII) or not present in *Youngina*. A small foramen for the facial nerve lies ventral to the crista prootica and just posterior to the incisura prootica (CN VII; Figs. 4A, 7B: VII). Its hyomandibular branch would have continued posteriorly, probably in a shallow recess ventral to the crista prootica

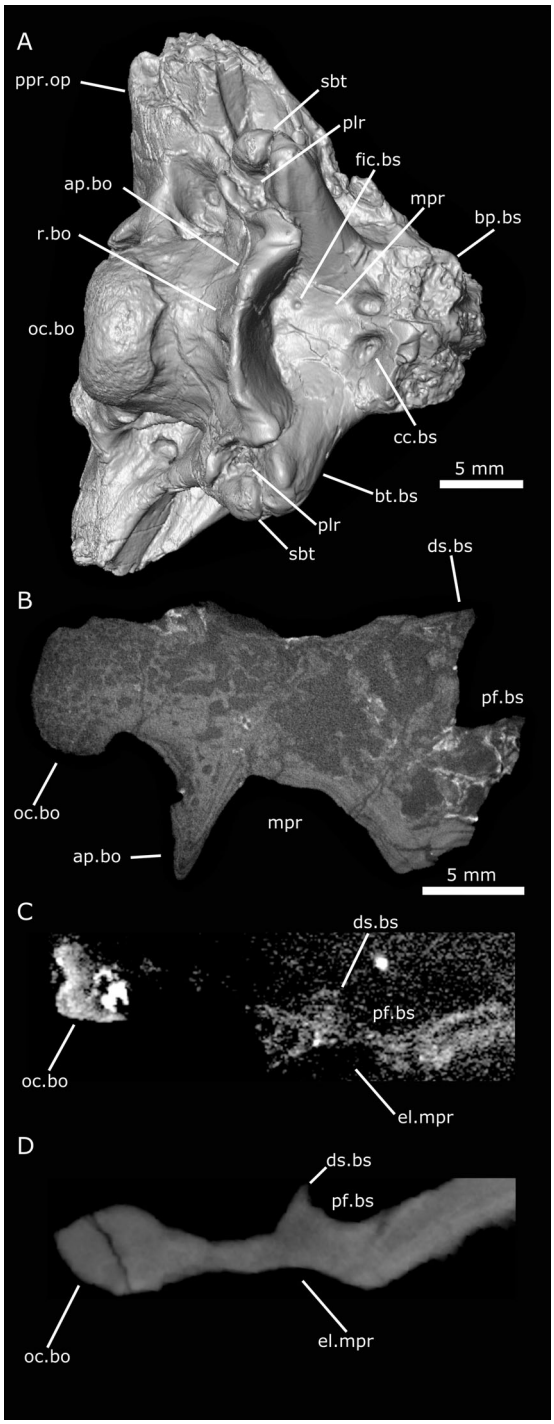

FIGURE 6. Details of median pharyngeal recess and cross section of *Trilophosaurus buettneri* and comparative specimens. **A**, *Trilophosaurus buettneri* specimen TMM 31100-443 in ventral view; **B**, *Trilophosaurus buettneri* specimen TMM 31100-443 midsagittal cross section; **C**, *Youngina capensis* specimen AMNH 5561 midsagittal cross section; **D**, *Mesosuchus browni* specimen SAM-PK 6536 midsagittal cross section. **Abbreviations**: **ap.bo**, anterior plate of basioccipital; **bp.bs**, basipterygoid process of parabasisphenoid; **bt.bs**, basitubera of parabasisphenoid; **cc.bs**, internal carotid canals through the parabasisphenoid; **ds.bs**, dorsum sellae of the parabasisphenoid; **el.mpr**, expected location of the median pharyngeal recess; **fic.bs**, possible foramen into parabasisphenoid; **mpr**, median pharyngeal recess; **oc.bo**, occipital condyle of basioccipital; **pf.bs**, pituitary fossa of parabasisphenoid; **plr**, pseudolagenar recess; **ppr.op**, paroccipital process of opisthotic; **r.bo**, ridge on the basioccipital; **sbt**, os sesamoideum basituberum (Element X).

(Oelrich 1956), whereas its palatine branch formed a shallow groove extending ventrally from the facial foramen. The configuration is similar to that of *Mesosuchus* and *Euparkeria*, whereas the path of VII in *Youngina*, *Macrocnemus*, and *Prolacerta* (Gow, 1975) is difficult to see beyond the initial foramen. A small but rugose process projects ventral to the crista prootica to separate the fenestra vestibuli from the facial foramen (Figs. 4B, 5B, 7B: vp.pr). This process is present in *Mesosuchus*, *Prolacerta*, and *Euparkeria* but apparently absent in *Youngina*, which again lacks a crista prootica. *Macrocnemus* bears a similar rugosity, but whether due to poor preservation or ossification, the *Macrocnemus* braincase lacks a clearly defined fenestra vestibuli and thus a clearly defined ventral process of the prootic (our observation of Miedema et al., 2020:fig. 5). The fenestra vestibuli of *Trilophosaurus* resembles that of *Prolacerta* and *Euparkeria* in being generally ovoid and intermediate in relative size between the larger foramen of *Youngina* and the smaller foramen of *Mesosuchus* (Fig. 4A, 7B: fv).

On the medial surface of the prootic, a shallow groove trends dorsally and posteriorly from the notch for the middle cerebral vein over the prominence of the anterior semicircular canal to the apex of the prootic (Fig. 4C: g.vcm). A relatively large fossa for the cerebellar flocculus (= floccular fossa or subarcuate fossa) (formed in part by the supraoccipital; Fig. 4C: ff.so) is present ventral to the notch for the middle cerebral vein. The floccular (subarcuate) fossa was noted in *Youngina*, *Mesosuchus*, *Prolacerta*, and *Euparkeria* and is figured but not described in *Macrocnemus* (our observation of Miedema et al., 2020:fig. 6B). The ampullary bulla occupies the triradiate suture between the prootic, supraoccipital, and opisthotic. Its wall is relatively thin, which is typical for the medial wall of the pan-archosaurian otic capsule (Fig. 4C: ab; Evans, 1986; Gower and Weber, 1998). Just anterior and ventral to the large ampullary bulla is an internal recess surrounding the exit foramen of CN VII (Fig. 4C: VII).

Supraoccipital—The supraoccipital is large relative to the other elements, with a quadrangular overall shape. It forms a broad, oblique contact with the prootics anterolaterally and a small contact with the opisthotics ventrolaterally (Figs. 2F, S5). In *Youngina*, *Macrocnemus*, *Mesosuchus*, *Prolacerta*, and *Euparkeria* the supraoccipital is oriented horizontally, whereas in *Trilophosaurus* it is a more vertical element. This orientation reflects the overall dorsoventral elongation characteristic of the *Trilophosaurus* braincase and skull. The supraoccipital forms the upper margin of the foramen magnum with a small lateral contribution from the paired opisthotics (Fig. 2B).

The anterior face of the supraoccipital is concave, arching anteriorly at the lateral edges to meet the prootic and opisthotic (Figs. 2A, 3C). From the medial concavity, the floccular fossa slopes laterally and ventrally (Fig. 4C: ff.so). Within the prootic facets are openings for the anterior semicircular canals and, more ventrally, the supraoccipital houses a portion of the vestibule (Fig. 4C: asc). A U-shaped process projects anteriorly and dorsally and likely contacted the parietals (Figs. 2A, 4C: up.so)—perhaps as a local autapomorphy of *Trilophosaurus*, although a similar morphology is present in *Azendohsaurus madagaskarensis* (Flynn et al., 2010). This region is damaged in TMM 31025-140 and TMM 31100-443. The U-shaped process reflects the continuation of a shallow, midline trough that begins approximately midway up the element's posterior surface (Fig. 2B). This posterior surface in TMM 31025-244 is marked by small, symmetrical depressions positioned where the dorsal head vein exits the braincase of *Mesosuchus*; in *Trilophosaurus* there is no external opening (Fig. 2B: ld.so; the depressions are absent in TMM 31025-140 and TMM 31100-443).

Opisthotic—The paired opisthotics contact the supraoccipital dorsomedially, exoccipitals ventromedially, and both the basioccipital and the os sesamoideum basituberum at the distal end of

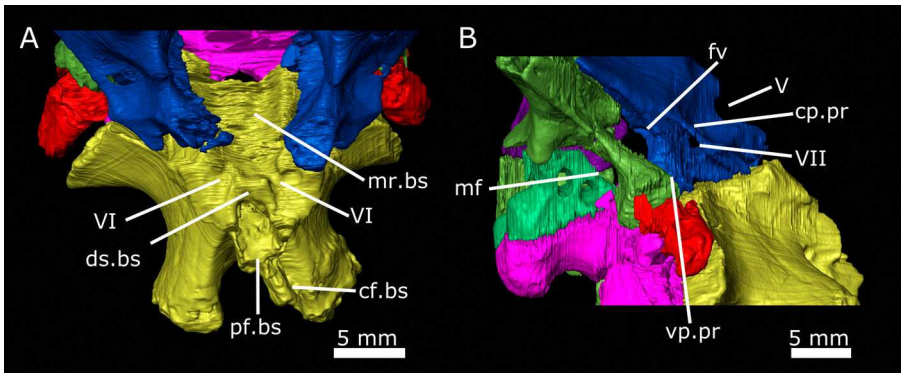

FIGURE 7. *Trilophosaurus buettneri* details of dorsal parabasisphenoid and posterolateral braincase. TMM 31025-244 in **A**, dorsal view; **B**, right posterolateral view with left prootic removed. **Abbreviations**: **cf.bs**, cultriform process of the parabasisphenoid; **cp.pr**, crista prootica **ds.bs**, dorsum sellae of the parabasisphenoid; **fv**, fenestra vestibuli; **mf**, metotic fissure; **pf.bs**, pituitary fossa, parabasisphenoid; **V**, CN V; **VII**, CN VII; **vp.pr**, ventral process of prootic.

its ventral ramus (Fig. S6). The ventral ramus remains separated from the posterolateral edge of the parabasisphenoid by the 'unossified gap' described above (Fig. 4B: ug; Gower and Weber, 1998). The ventral ramus is distinctly club-shaped (Fig. 4A: vr.op) as it is in *Mesosuchus* and *Prolacerta*, and more pronounced than in *Euparkeria*; in *Macrocnemus*, the process is expanded but not like a club, whereas in *Youngina* the ramus is thinner and rod-like. The opisthotic forms most of the paroccipital process (Fig. 2C, D: ppr.op), which projects posterolaterally to contact the squamosals laterally. Their anteroventral surface bears a stapedial recess (Fig. 4A: sr).

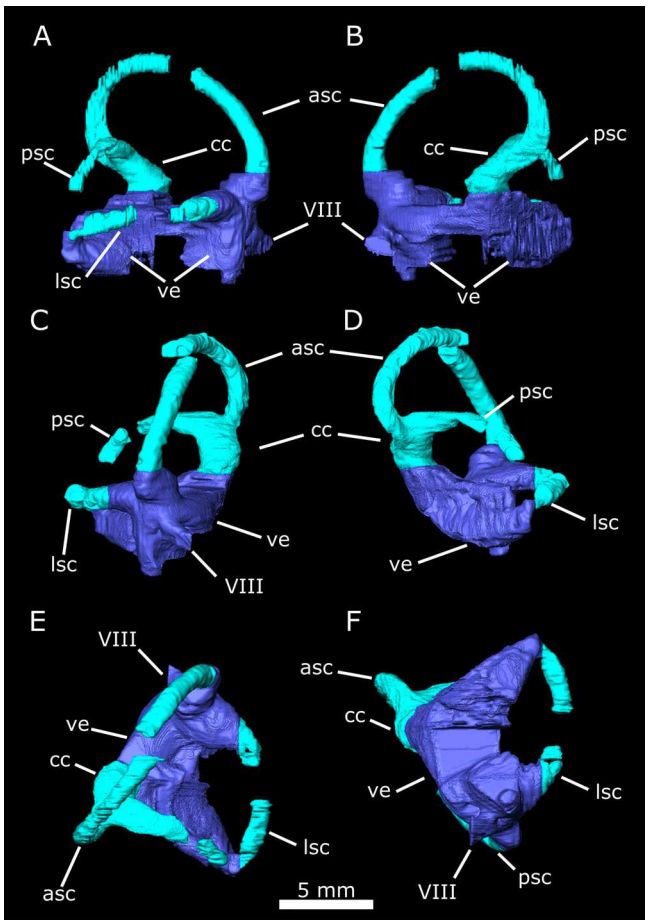

FIGURE 8. *Trilophosaurus buettneri* TMM 31025-244 right inner ear endocast in **A**, lateral view; **B**, medial view; **C**, anterior view; **D**, posterior view; **E**, dorsal view; **F**, ventral view. **Abbreviations**: **asc**, anterior semicircular canal; **cc**, common crus; **lsc**, lateral semicircular canal; **psc**, posterior semicircular canal; **ve**, vestibule of the inner ear; **VIII**, CN VIII.

Stapes—Only TMM 31025-140 preserves the stapes, and although largely incomplete, it is *in situ* on the right side (Gregory, 1945; Parks, 1969). The footplate fills the vestibular window with a somewhat gracile shaft. The stapedial morphology compares closely to that of *Mesosuchus*, which was interpreted as transmitting only low-frequency sounds (Sobral and Müller, 2019).

Os sesamoideum basituberum (Element X)—This is a paired, stout, rod-like bone that, in all three of the examined *Trilophosaurus* specimens, is positioned just behind the basitubera, contacting the basioccipital laterally and posteriorly, the opisthotic dorsally, and the parabasisphenoid anteriorly (Figs. 2, 5A, B). It is possible that the element represents a region of the basitubera with a tendency for breakage and thus should not be considered an independent bone. However, the element shares long contacts with both the basisphenoid and basioccipital that are not obviously conducive to consistent breakage and bilateral breakages are highly unlikely although not impossible. A cross-sectional fracture with the opisthotic would seem more likely; but here the interface between the os sesamoideum basituberum and the overlying opisthotic is thick and again not an obvious point of weakness where one would predict consistent fracture. For these reasons, we agree with Parks (1969) that the os sesamoideum basituberum can be hypothesized as an independent bone representing the ossified tendon of a head flexor. This may have formed within the tendon itself or as a traction epiphysis, but either origin results in what is often called a sesamoid (Gauthier et al., 2012, Montero et al., 2017). We agree with Merck (1997) that the identity of the head flexor is m. rectus capitis anterior rather than m. longissimus capitis based on the former's more ventrolateral insertion on the archosaurian basituberum (Tsuihiji, 2007).

The structural independence of the os sesamoideum basituberum from other neurocranial elements may not be the most important point here. If, for example, the os sesamoideum basituberum represents a broken fragment of an elongate opisthotic process that contributes to the basituberal process, this would still represent a derived morphology for Pan-Archosauria. Such a process may well be the derived product of a membranous co-ossification of the m. rectus capitis anterior tendon with the endochondral cranial base as opposed to a derived elongation of the posterior otic capsule (the cartilaginous precursor to the opisthotic proper). Bony processes commonly have such an origin (Vargas et al., 2017), and the developmental dynamics between head flexors and this region of the basicranium might also be the source of variation in the shape of the descending process of the opisthotic described above and considered with phylogenetic results (below). In its most distilled form, our argument is

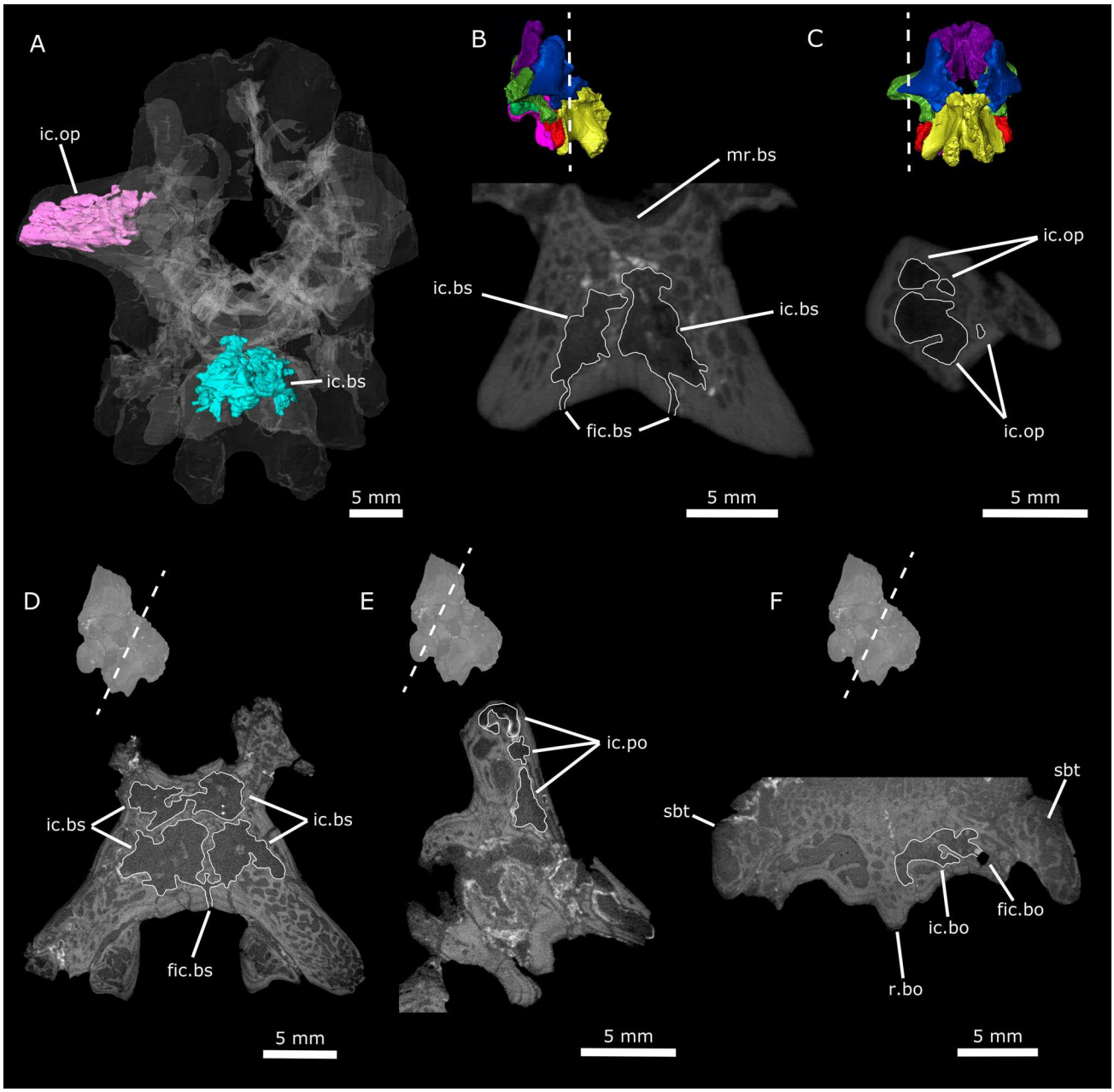

FIGURE 9. *Trilophosaurus buettneri* details of internal cavities. **A**, TMM 31025-244, braincase rendered transparent with cavities in opisthotic and basioccipital in pink and blue, respectively; **B**, TMM 31025-244, coronal section through parabasisphenoid with internal cavity and foramina in parabasisphenoid outlined in white; **C**, TMM 31025-244, sagittal section through paroccipital process with internal cavity in opisthotic outlined in white; **D**, TMM 31100-443, section through parabasisphenoid with internal cavity and foramen outlined in white; **E**, TMM 31100-443, section through prootic with internal cavity outlined in white; **F**, TMM 31100-443, section through basioccipital with internal cavity outlined in white. **Abbreviations**: **fic.bo**, possible foramen into open space in basioccipital; **fic.bs**, possible foramen into open space in parabasisphenoid; **ic.bs**, internal cavity in the parabasisphenoid; **ic.op**, internal cavity in the opisthotic; **ic.po**, internal cavity in the prootic; **mr.bs**, medial ridge of the parabasisphenoid; **r.bo**, ridge on the posterior face of the basioccipital; **sbt**, os sesamoideum basituberum (Element X).

that *Trilophosaurus* expresses a derived pattern of basituberal ossification that can be referred to as the os sesamoideum basituberum and that we hypothesize originates as a tendinous ossification.

Inner Ear—The right inner ear cavity of TMM 31025-244 is nearly complete (Fig. 8), whereas the left is only partially preserved; where the preservation of the two sides overlaps, their morphology agrees. On both sides, preservation prevented segmentation of the lagena, although what is discernible does not suggest a morphology that differs from that expected for a stem archosaur (Hanson et al., 2021). All three semicircular canals circumscribe an approximately ovoid arc, with the posterior and lateral canals being approximately the same length. The anterior semicircular canal is more elongate, rising well above the common crus (Fig. 8). Despite this derived length, the anterior canal retains the plesiomorphic shape found in *Youngina*, *Mesosuchus*, and *Euparkeria* (see Discussion). The medial wall of the

vestibule is well preserved dorsally where it includes an anteriorly positioned vestibulocochlear foramen (CN VIII). Limited ventral ossification of this wall means that the lower extent of this vestibule must be estimated. In these features, *Trilophosaurus* is similar to *Youngina* and other early pan-archosaurs.

Other Cavities—All braincase bones have an internal structure that couples a relatively thick rind of cortical bone with numerous small, cell-like internal cavities—a combination also present in *Mesosuchus* and *Euparkeria* (Sobral et al., 2016). The same bones in crown lepidosaurs also contain networks of internal cavities and these actually constitute a larger percentage of the overall internal volume of their respective bones than in early pan-archosaurs. This disparity reflects the fact that, relative to squamates, the outer layer of compact bone in the pan-archosaur fossils is thicker and there is more extensive ossification within the deep cancellous region (i.e., the individual cell-like cavities are more clearly defined in bone). In this sense, the pan-archosaur condition compares more closely to that of *Youngina* and turtles (our observations of AMNH 5561 and several turtles including, for example, *Claudius angustatus*).

An important distinction between the *Trilophosaurus* condition and that of *Youngina*, squamates, and turtles is the additional presence of larger, internal cavities that communicate via canals with the bone surface and thus the extracranial space. This is especially notable given that an external communication is a criterion for identifying the incorporation of pneumatic diverticula within the bony structure of fossils (pneumatization; Witmer, 1990). If the *Trilophosaurus* neurocranium is pneumatized, then it represents an early, if not the earliest, example of pneumatization in Pan-Archosauria. Thus, the details here are critical.

The largest internal cavity (Fig. 9A, B, D) lies in the midline of the parabasisphenoid and corresponds positionally to the basisphenoid (subsellar) recess of pan-avians (Witmer and Ridgely, 2009) and basisphenoid diverticulum of the median pharyngeal sinus system of crocodilians (Dufeau and Witmer, 2015). In TMM 31025-244, this space communicates ventrally with the median pharyngeal recess through a pair of slit-like openings that are both dorsoventrally and anteroposteriorly long. These openings lie on either side of the median sagittal plane and open ventrally within the basisphenoid's contribution to the roof of the median pharyngeal recess. The external openings do not express as foramina, per se, but rather as somewhat irregular fissures. This external signature presents more like damage than a natural opening. A physiological/anatomical origin, however, is supported by their paired nature, the bilateral symmetry of their length and position, and their collective location within the deepest part of the median pharyngeal recess (where the geometry of the skull is not obviously conducive to the necessary form of breakage). Although it is difficult to describe with precision, the internal lengths of these openings also appear more natural (less jagged) than their external apertures.

The same parabasisphenoid cavity is also present in TMM 31025-140 and TMM 31100-443. In the former, the cavity lacks any clear external opening, but data quality here is poor and the parabasisphenoid is heavily damaged. In TMM 31100-443, the cavity communicates with the extracranial space via a single foramen in the parabasisphenoid positioned just to the right of its sagittal midline (Fig. 6A). The basisphenoid cavity in TMM 31100-443 compares closely with that of TMM 31025-244 in being partitioned into right and left subcavities in the region dorsal to their external openings. In TMM 31025-244, these paired subcavities communicate with the median pharyngeal recess via individual canals, whereas in TMM 31100-443 each subcavity has a short, bilaterally symmetrical canal that extends ventromedially. These internal canals join to form a single, relatively long canal that approximates the sagittal midline and extends ventrally to the aforementioned single parabasisphenoid foramen.

The parabasisphenoid of *Mesosuchus* also contains several large internal cavities. One communicates with the subcranial space through foramen-like openings directed ventrolaterally, but differs from that of *Trilophosaurus* in being more posteriorly positioned and paired, with no midline confluence. They primarily lie within the basitubera but do approach the sagittal midline. The anterior and lateral margins of these openings are well delineated in bone and have a rounded appearance, whereas their posteromedial margins are confluent with a space appearing to represent the poorly ossified contact between the parabasisphenoid and basioccipital. Unlike in the *Trilophosaurus* openings, these foramina are not connected to their internal cavities by an elongate canal circumscribed by bone but rather open directly into the cavity itself. That this disparity reflects the poorly ossified nature of this area in *Mesosuchus* is a possibility. Other internal cavities in the parabasisphenoid of *Mesosuchus* without associated foramina include a paired cavity that invades the basipterygoid processes and a midline cavity in the cultriform process.

A second large cavity in *Trilophosaurus* lies within the opisthotic, at the base of the paraoccipital process (Figs. 2D, 9A, C). This space corresponds to that occupied by the caudal tympanic recess in pan-avians (Witmer and Ridgely, 2009) and the otoccipital diverticulum of the pharyngotympanic sinus system of crocodilians (Dufeau and Witmer, 2015). Evidence that these *Trilophosaurus* cavities are pneumatic in origin is relatively weak as we cannot confirm associated external foramina; however, the poor preservation of this region in each of the specimens does not permit a confident statement that foramina were absent. The base of the paraoccipital process in *Mesosuchus* contains an enlarged internal cavity that lacks obvious external foramina (Sobral and Müller, 2019).

The paired prootics each house an enlarged internal cavity that is confluent with adjacent smaller internal cavities of the supraoccipital but that fails to meet its contralateral partner along the midline. These prootic cavities are most clearly defined in TMM 31100-443 (Fig. 9E) but are present in TMM 31025-244 and on the right side in TMM 31025-140, though data quality does not allow confirmation in the left side of TMM 31025-140. Positionally, the spaces correspond to the rostral tympanic recess or part of the caudal tympanic recess of pan-avians (Witmer and Ridgely, 2009) and the intertympanic diverticulum or prootic diverticulum of the pharyngotympanic sinus system of crocodilians (Dufeau and Witmer, 2015). Again, there are no openings connecting the *Trilophosaurus* cavities to the extracranial space that are unquestionably natural. Openings exist in both TMM 31100-443 and TMM 31025-244 but are more likely fractures than anatomical foramina/canals. Whether this damage is obscuring clearly anatomical openings cannot be determined with confidence.

The last internal cavity of note lies in the basioccipital of TMM 31100-443. At the base of the tab of the basioccipital is a foramen which opens into a small cavity that is confined to the right side of the specimen (Fig. 9F). On the left side of TMM 31100-443 there appears to be a small depression on the basioccipital tab, but damage obscures any potential canal to the interior of the bone. There are small, interconnected spaces in this part of the basioccipital of TMM 31025-244 and TMM 31025-140, but no apparent foramina opening into those cavities. Positionally, this space is homologous to the medial subcondylar recess of pan-avians and the basioccipital diverticulum of pan-crocodilians (Witmer and Ridgely, 2009; Dufeau and Witmer, 2015). *Mesosuchus* and *Euparkeria* both have cavities in the basitubera, although in both those taxa the cavities are larger than in *Trilophosaurus* and the spaces themselves lie laterally. In *Mesosuchus* (uncertain for *Euparkeria*), the foramina opening into the basituberal cavities are anterior to the basitubera, rather than posterior to the basitubera as we find in *Trilophosaurus*.

Phylogenetic Analysis

Our data support alternative scorings of *Trilophosaurus* for seven published characters. These include: (1) fusion of exoccipital to opisthotic or other braincase elements (from fused to the opisthotic to variable; Ezcurra, 2016 and Scheyer et al. 2020, 211; Stocker et al., 2016, 62; Pritchard et al., 2018, 61; Pritchard and Sues, 2019, 99), (2) ventral contralateral contact of exoccipitals (from present to absent; Stocker et al., 2016, 61; Pritchard et al., 2018, 60; Pritchard and Sues, 2019, 98), (3) ventral ramus of opisthotic, shape (from rod-like and very robust to club-shaped; Ezcurra, 2016 and Scheyer et al., 2020, 217), (4) semilunar depression (from present to absent; Ezcurra, 2016 and Scheyer et al., 2020, 238; Stocker et al., 2016, 62; Pritchard et al., 2018, 209; Pritchard and Sues, 2019, 108), (5) posterior face of occipital condyle (variable between 'pinprick' notochordal pit and convex; Pritchard et al., 2018, 63; Pritchard and Sues, 2019, 100), (6) median pharyngeal recess (from absent to present; Ezcurra, 2016 and Scheyer et al., 2020, 239), and (7) 'pseudolagenar recess' (from absent to present; Ezcurra, 2016 and Scheyer et al., 2020, 223).

We also assessed nine characters left unscored in Ezcurra (2016) and a further two characters in the updated version of that matrix analyzed by Scheyer et al. (2020), including: (1) parabasisphenoid exposure at midline of endocranial cavity (present; Ezcurra, 2016 and Scheyer et al., 2020, 234:0), (2) parabasisphenoid, anterior tympanic recess (absent; Ezcurra, 2016 and Scheyer et al., 2020, 245:0), (3) floccular fossa (extends onto internal surface of supraoccipital; Ezcurra, 2016 and Scheyer et al., 2020, 249:1), (4) contralateral contact of prootics (absent; Ezcurra, 2016 and Scheyer et al., 2020, 253:0), (5) lateral face of prootic (crista prootica present; Ezcurra, 2016 and Scheyer et al., 2020, 254:1), (6) prootic, anterior inferior process (well-developed; Ezcurra, 2016 and Scheyer et al., 2020, 255:1), (7) prootic, ridge on lateral surface of anterior inferior process (present; Ezcurra, 2016 and Scheyer et al., 2020, 256:0), (8) medial wall of vestibule (incompletely ossified; Ezcurra, 2016 and Scheyer et al., 2020, 257:0), (9) laterosphenoid ossification (absent; Ezcurra, 2016 and Scheyer et al., 2020, 258:0), (10) prootic contribution to paroccipital process (contributes; Scheyer et al., 2020, 645:1), and (11) anterior inferior and superior processes of prootic (well separated; Scheyer et al., 2020, 694:0).

Our analysis of the Ezcurra (2016; 40 MPTs, 2649 steps, CI = 0.298, RI = 0.624), Scheyer et al. (2020; 27 MPTs, 3868 steps, CI = 0.240, RI = 0.646), Stocker et al. (2016; 5 MPTs, 622 steps, CI = 0.420, RI = 0.642), and Pritchard et al. (2018; 2 MPTs, 1099 steps, CI = 0.327, RI = 0.645) resulted in no change to the preferred topologies of the original authors. Bremer indices calculated in TNT (v 1.5; TBR on existing trees retaining trees suboptimal by 15 steps) showed limited differences from Bremer indices calculated on the original matrices. In the altered Ezcurra (2016) analysis there was no change in support for any branches of the tree. In the altered Scheyer et al. (2020) analysis there was a reduction in support of (*Pamelaria dolichotrachela* + (*Shringasaurus indicus* + *Azendohsaurus*)) from a Bremer index of 5 to 4 and a reduction in support of (*Shringasaurus indicus* + *Azendohsaurus*) from a Bremer index of 3 to 2. In the altered Stocker et al. (2016) analysis there was a reduction in support for (*Teraterpeton hrynewichorum* + (*Trilophosaurus buettneri* + (*Spinosuchus caseanus* + *Trilophosaurus jacobsi*))) from a Bremer index of 2 to 1. In the altered Pritchard et al. (2018) analysis there was an increase in support for Squamata from a Bremer index of 1 to 2.

Several hypotheses of stem archosaur relationships do shift in our analysis of the altered Pritchard and Sues (2019; 6 MPTs, 1217 steps, CI = 0.306, RI = 0.645) apparently driven by scoring the semilunar depression as absent and the occipital condyle as polymorphic for having a convex shape and bearing a small notochordal pit. These include a *Protorosaurus*-Tanystropheidae clade as sister to all other pan-archosaurs, Trilophosauridae (sensu Pritchard and Sues, 2019) as sister to a *Boreopricea*-kuehneosaur clade, and the combined Trilophosauridae-*Boreopricea* clade as sister to a Rhynchosauridae-everything crownward clade. The azendohsaurids, *Pamelaria dolichotrachela*, and *Shringasaurus indicus* (with *S. indicus* rather than *P. dolichotrachela* as the first-diverging taxa in that lineage) are together removed from their close relationship with the trilophosaurids and moved crownward as sister to Archosauriformes (Fig. S7). Bremer indices calculated in TNT (v 1.5; TBR on existing trees retaining trees suboptimal by 15 steps) show that most clades have similar levels of support, whereas the shift of azendohsaurids, *P. dolichotrachela*, and *S. indicus* crownward increases the Bremer support value of that clade from 3 to 6, and both Archosauromorpha and Lepidosauromorpha have support indices increased from 2 to 3.

We also added the absence (0)/presence (1) of an elongated anterior semicircular canal to the matrix of Stocker et al. (2016). The state of this feature remains unknown for a majority of tip taxa, but we were able to score *Youngina capensis* (0), *Shinisaurus crocodilurus* (0), *Trilophosaurus buettneri* (1), *Mesosuchus browni* (0), *Proterosuchus fergusi* (0), *Prolacerta broomi* (0), *Euparkeria capensis* (0), and *Triopticus primus* (1) (scorings based on Bever et al., 2005; Sobral et al., 2016; Brown et al., 2019; Sobral and Müller, 2019; Hanson et al., 2021). Adding this character to our analysis (7 MPTs, 624 steps, CI = 0.420, RI = 0.642) further erodes what was already a poorly resolved tree leaving *Trilophosaurus* as part of a large polytomy that includes crown archosaurs (Fig. S8).

DISCUSSION

The above descriptions integrate a small set of phylogenetically strategic comparisons in order to establish basic polarity hypotheses for the *Trilophosaurus* phenotype. Here we expand on these comparisons for selected characters and discuss how neurocranial morphology informs our understanding of both the unique biology of *Trilophosaurus* and potential transformations within the more inclusive early history of Pan-Archosauria. These discussions include both a review of neurocranial autapomorphies in *Trilophosaurus* and a more general review of additional neurocranial synapomorphies, including pneumatization. These discussions are not meant as comprehensive but represent observations based on a broad, but not particularly dense, sampling of major reptile clades. This sample includes the captorhinids *Labidosaurus hamatus* (Modesto et al., 2007), *Captorhinus aguti* (Price, 1935; Fox and Bowman, 1966), *Eocaptorhinus laticeps* (Heaton, 1979), and *Captorhinus kierani* (DeBraga et al., 2019); *Petrolacosaurus kansensis* (Reisz, 1981); the varanopids *Aerosaurus wellesi* (Langston and Reisz, 1981) and *Varanops brevirostris* (Campione and Reisz, 2010); the parareptiles *Milleretta rubidgei*, *Milleropsis pricei* (Gow, 1972), *Procolophon trigoniceps* (Carroll and Lindsay, 1985), *Deltavjatia rossicus* (Tsuji, 2013), *Mesosaurus tenuidens* (Modesto, 2006), *Leptopleuron lacertinum* (Spencer, 2000), and *Belebey vegrandis* (Reisz et al., 2007); *Claudiosaurus germaini* (Carroll, 1981); the pan-lepidosaurs *Simosaurus gaillardoti*, *Nothosaurus* sp. (Rieppel, 1994), *Placodus gigas* (Neenan and Scheyer, 2012), *Sphenodon punctatus* (Evans, 2008), *Ctenosaura pectinata* (Oelrich, 1956), and *Shinisaurus crocodilurus* (Bever et al., 2005); the stem turtle *Proganochelys quenstedti* (Gaffney, 1990); and the pan-archosaurs *Erythrosuchus africanus* (Gower, 1997) and *Euparkeria capensis* (Gower and Weber, 1998; Sobral et al., 2016). Throughout these discussions, we only mention taxa when the character in question is scorable. Our

hope is that these observations serve as a useful platform for more directed braincase studies, analyses, and reviews.

A number of characters exhibit variation that is especially difficult to understand in terms of either phylogeny or function. These include: number of hypoglossal foramina, ventral projection of the prootic below the crista prootica, ossification of the fenestra vestibuli, unossified gap/lagenar recess, medial ridge on the braincase floor, orientation of the basipterygoid processes, parasphenoid crests, branching of CN VII after leaving the braincase, morphology of the basitubera, orientation of the parabasisphenoid/prootic facets, articulation of the parabasisphenoid/basioccipital, and anterior-inferior process of the prootic. Much of this variation is likely the product of late-stage ontogenetic transformations that is difficult to fully understand in a fossil record characterized by low sample sizes. A full review of these characters is beyond the scope of our study but represents a wide-open field of questions for the increasing body of reptilian researchers. Focused, character-based study should be used to sharpen character identities and clarify the diagnosis of those characters across clades and will undoubtedly assist our understanding of reptilian evolution.

Trilophosaurus Neurocranial Autapomorphies

Inner Ear and Locomotion—Arguably the most intriguing of the neurocranial features that optimizes as autapomorphic for *Trilophosaurus* is its distinctly elongated anterior semicircular canal. This morphology is most closely associated with theropod dinosaurs (Georgi et al., 2013) where it was considered a potential adaptation of bipedality (Witmer and Ridgely, 2009). The similarity between the *Trilophosaurus* and theropod inner ears is so striking that a phylogenetic analysis using ear shape alone by Ezcurra et al. (2020) nested *Trilophosaurus* among the theropods. The association of bipedality and a distinctly elongated anterior semicircular canal among crown archosaurs extends beyond theropods and likely distributes all the way to the base of Pan-Aves (Hanson et al., 2021). A smaller degree of elongation for the anterior canal appears to characterize the ancestral crown archosaur based on the inner-ear morphology of Phytosauria (Lautenschlager and Butler, 2016). This is the case regardless of whether phytosaurs represent the earliest-diverging clade within Pan-Crocodylia (Ezcurra, 2016) or just outside crown Archosauria (Nesbitt, 2011).

An obvious question is whether the independently acquired elongate anterior semicircular canal indicates bipedality in *Trilophosaurus*? The possibility that *Trilophosaurus* was bipedal received early attention by Gregory (1945) who concluded that it could not have been bipedal, at least in the sense that theropods are. This conclusion was based on the relative lengths of the humerus/femur and the low neural spines on the vertebrae. It was noted by Georgi et al. (2013) that, in addition to the elongate anterior canal, the ear of bipedal archosaurs exhibits an elongate lateral canal, and both derived features may be necessary for a fully bipedal ecology. The length of the lateral canal of *Trilophosaurus* compares closely with that of the posterior canal and is thus lacking this derived, potentially bipedal, signature.

In his discussion, Gregory (1945) conceded that *Trilophosaurus* may have enjoyed some form of derived functionality, including the ability to rear onto its hind legs. He also proposed that *Trilophosaurus* was arboreal, using as evidence the highly recurved tips of its claws. This behavioral potentiality received subsequent support in Spielmann et al. (2005), which considered claw morphology, length ratios of the manus and pes relative to the trunk, humeral morphology, and pectoral girdle morphology. These observations are based largely on direct comparisons of measurements and ratios between species rather than quantitative and statistical analyses. Other analyses (Jenkins et al., 2020) suggest that claws of arboreal species tend to be deeper relative to their length than in species that use other substrates, and this conforms to the general shape of the *Trilophosaurus buettneri* claw, but further measurement and analysis directly measuring *Trilophosaurus* specimens is needed. In addition to their other considerations, Spielmann et al. (2005) note that in congruence with many climbing tetrapods, the first digit of *Trilophosaurus* diverges medially from the other digits. This divergence is not the full opposition found in many arboreal taxa (Zhou et al., 2021), and the relevance of this point is difficult to assess without data directly addressing the efficacy of such an intermediate autopodal morphology for climbing in a relatively large-bodied taxon. More generally, the form-function relationship across this type of evolutionary transition is often imprecise, which complicates paleobiological inferences (Lauder, 1995).

Without well-established correlations between vestibular morphology and arboreality, our inner ear data are mute on whether *Trilophosaurus* spent time in trees. Indeed, recent criticisms of the connection between semicircular canal shape and locomotor function suggest any predictive power of canal shape is no better than chance (David et al., 2022 in comment on Hanson et al., 2021), although a well-established form-function pattern remains across taxa (Hanson et al., 2022 in reply to David et al., 2022). Its elongate anterior semicircular canal may support a derived level of agility (see Spoor et al., 2007) that may be necessary for arboreality but that could have served *Trilophosaurus* in a myriad of ways, possibly including advanced forms of locomotion. If *Trilophosaurus* was indeed incapable of a theropod-like bipedality, then any pan-avian correlation between that modality and an elongate anterior canal would not hold for the entirety of the archosaur stem lineage. Considering this pattern, the hesitation of Stocker et al. (2016) to assign bipedality to *Triopticus primus*, the only other stem archosaur known to have an elongate anterior semicircular canal (acquired independent of both crown archosaurs and *Trilophosaurus*), seems prudent.

Os sesamoideum basituberum (Element X)—We interpret the small ossification lying adjacent to the basioccipital-parabasisphenoid suture as the ossified tendon of the m. rectus capitus anterior (Merck, 1997). This is in general agreement with the interpretation of Parks (1969) who considered it to be the ossified tendon of the m. longissimus capitus. Both muscles are ventroflexors of the head (Snively and Russel, 2007), so the disagreement in tendon identity is unlikely to bear much if any functional significance. The m. rectus capitus anterior of crown archosaurs attaches to the basisphenoid more ventrolateral to the attachment of the m. longissimus capitus (Tsuihiji, 2007), and thus in a more comparable position to the os sesamoideum basituberum.

Although Parks (1969) referred to this bone as 'X,' there is no evidence that he was equating it in any way with 'Element X' of amphisbaenians—a name that appears to enter the literature in Zangerl (1944). It seems likely that Parks was unaware of the amphisbaenian element (and name) as he failed to mention it despite noting the presence of an unnamed ossification in the iguanid squamate *Ctenosaura pectinata*, citing the classic description of Oelrich (1956). The amphisbaenian 'Element X' is a regular ossification that lies adjacent to the basioccipital-parabasisphenoid suture in these largely fossorial animals (see Gans and Montero, 2008). The bone is hypothesized to strengthen the insertion of powerful muscles used to flex the head upon the neck while burrowing (Montero et al., 2017), in part due to the higher ultimate tensile stress of ossified tendon than bone or tendon alone (Currey, 1999; Organ, 2006). It is increasingly clear that a positionally homologous ossification is widely distributed among squamates, to the extent that it may even be plesiomorphic for the squamate crown clade (Montero et al., 2017). While such a distribution may dilute the diagnostic value of the bone in terms of detailed function/behavior (beyond relatively

strong head flexion), it increases the possibility that the ossification in this area, or at least the tendency of tissues in this area to ossify, has an even deeper history that includes the early diversification of other reptilian lineages (including Pan-Archosauria). It is thus important that the anatomical nomenclature reflects this potentiality and the primary homology (sensu de Pinna, 1991) it represents. Simply stated, we use connectivity to argue that any phylogenetic matrix for Reptilia that includes the presence of this ossification should score the squamate and *Trilophosaurus* condition as equivalent (i.e., having primary homology). This practice recognizes homology as the null hypothesis and assures that this shared connectivity is allowed to influence the tree topology and thus the evidence for secondary homology (see the pneumatization section below for a parallel discussion of homology that includes further conceptual details). Failure to do so erodes our ability a priori to recognize a broadly conserved developmental potential should one exist.

Although we are hesitant to upset an established literature based around the name 'Element X,' it may be appropriate to employ a more descriptive anatomical name. This is especially true if it is likely to be recognized outside of the squamate lineages where 'Element X' is commonly employed by specialists. The bone was referred to by Gauthier et al. (2012) as an 'apophyseal ossification' but we follow the interpretation that the ossification is a sesamoid, regardless of later fusion to the braincase in some amphisbaneans (although these definitions are not mutually exclusive, see Montero et al., 2017). We advance the name os sesamoideum basituberum given its origin as an intratendinous ossification among squamates, and the position near the basitubera where it is consistently found (Montero et al., 2017).

That the expression of os sesamoideum basituberum reflects powerful head flexion in *Trilophosaurus* is reinforced by the expanded nature of the vertical, basioccipital plate that buttressed the basitubera against posteriorly directed forces (Gregory 1945). This feature is shared among described stem archosaurs only with *Azendohsaurus madagaskarensis* (Flynn et al., 2010), a taxon that apparently lacks this ossification. More directed studies on the conditions under which these flexor tissues ossify and the functional and evolutionary implications of this potential are needed.

Medial Cerebral Vein—Among pan-reptiles, the medial cerebral vein (= transversotrigeminal vein, Porter and Witmer, 2015) and the root of the trigeminal nerve tend to exit the neurocranium through a shared incisura prootica. Partitioning of this space so these structures traverse the primary neurocranial wall through separate openings is a derived condition found scattered across the tree. Exemplar taxa include the early stem reptile *Captorhinus aguti* (Heaton 1979), the sauropterygian *Placodus gigas* (Neenan and Scheyer, 2012), and amongst various crown Lepidosauria (e.g., *Ctenosaura pectinata;* Oelrich, 1956). The partitioned condition is also present in some crocodile-line crown archosaurs (e.g., *Stagonolepis robertsoni*; Walker, 1972, and *Desmatosuchus haploceras*; Small, 2002) as is a partially divided morphology (e.g., *Sphenosuchus acutus*; Walker, 1990). The plesiomorphic common exit is dominant among early pan-archosaurs (see Nesbitt, 2011) and we know of no stem archosaurs, besides *Trilophosaurus*, that exhibit the fully partitioned condition. Care should be taken with this and similar characters given that the neurocranium continues to ossify late in postnatal ontogeny such that variation in the extent of chondral ossification should be expected even among individuals otherwise considered skeletally mature (e.g., Bever 2009a, b).

Other Possible Autapomorphies—A distinct neck separating the occipital condyle from the main body of the basioccipital was scored and described by Ezcurra (2016). The *Trilophosaurus* version of this feature is especially obvious in lateral view and appears to be autapomorphic among early stem archosaurs. Ultimately, this character would benefit from a more robust shape analysis as variations and intermediate states are common across Pan-Reptilia.

We also advocate a careful survey of the braincase floor with regards to the relative contributions of the basioccipital and parabasisphenoid (considered without the dermal cultriform process). It is unclear how these contributions are patterned, but most crown diapsids exhibit a relatively large parabasisphenoid. Variations on this condition exist in all the major lineages—e.g., see *Ctenosaura pectinata* among crown squamates; *Eunotosaurus africanus* and *Proganochelys quenstedti* among stem turtles (Oelrich, 1956; Gaffney, 1990; Bever et al., 2015). The relatively large basioccipital contribution in *Trilophosaurus* may reflect the more general anteroposterior shortening of its braincase and skull. However, similar proportions within the ossified basal plate are present in more crownward pan-archosaurs such as *Erythrosuchus africanus* and *Euparkeria capensis* (but not, e.g., *Mesosuchus*; Gower, 1997; Sobral et al., 2016). It is thus possible that the *Trilophosaurus* condition may be more broadly synapomorphic within the pan-archosaur radiation.

Additional Character Discussions

Crista Prootica—Despite some mention in the literature of early pan-reptiles (e.g., Heaton, 1979), the crista prootica is not a consistent feature of the early eureptilian or parareptilian braincase and is absent or unknown among diapsid stem saurians. It is present in both the lepidosaurian and archosaurian crown groups (Currie, 1997; Gauthier et al., 2012), but like so many characters, its homology across the collective saurian crown is clouded in part by the poorly understood nature of the lepidosaurian stem. Among sauropterygians, the crest is generally absent but not altogether unknown (Sato et al., 2011). It is lacking among crown turtles (Gaffney, 1979), present in some stem turtles such as *Proganochelys quenstedti* (see also Bhullar and Bever, 2009) and possibly *Kayentachelys aprix* but remains unknown for the basally branching pan-turtles *Eorhinochelys* (Li et al., 2018), *Odontochelys* (Li et al., 2008), *Pappochelys* (Schoch and Sues, 2018), and *Eunotosaurus* (Bever et al., 2015). Current evidence suggests the crista prootica is a crown saurian feature that was likely subject to considerable homoplasy especially in the early history of the radiation.

Reduction/Absence of Notochordal Pit—A notochordal pit is expressed widely among early pan-reptiles including captorhinids, parareptiles, *Petrolacosaurus kansensis*, and varanopids. The primitive form of this feature (i.e., as found in *Youngina*) is largely absent among pan-lepidosaurs, although many lepidosaurs have a concave occipital condyle whose shape may well reflect the notochord's influence on the ossifying basal plate. The situation is much the same among pan-archosaurs where the wholly primitive form of the pit is unknown (at least to us) but where many taxa exhibit variations that likely represent a notochordal signature on the occipital condyle. *Erythrosuchus africanus*, for example, exhibits a narrow, vertically oriented concavity, whereas all evidence of the notochord is obliterated in the convex condyle of *Euparkeria capensis*. Variation among the three examined specimens of *Trilophosaurus* supports the hypothesis that the developmental relationship between notochord and occipital condyle is relatively 'loose' in this area of the tree. If the associated morphology continues to transform late in post-natal ontogeny, then this variation might reflect slight age differences between the specimens and/or an ancestral polymorphism that eventually gave way to a more consistently closed condition. This character needs more directed study, especially given its influence in some archosaurian matrices (e.g., Pritchard and Sues, 2019). Despite its common expression among both crown and stem turtles (Gaffney, 1979, 1990), we conclude that the reduced state of

the pit in *Trilophosaurus* is most likely derived at the reptilian node rather than within Pan-Archosauria; considerable homoplasy/polymorphism may again describe the early reptilian history of this character.

Ventral Ramus of the Opisthotic—In the reptilian total group the ventral ramus of the opisthotic is plesiomorphically a stout rod sutured to the lateral part of the basioccipital and exoccipital. The rod-shaped morphology is generally present in the captorhinids, *Petrolacosaurus kansensis*, the varanopids, and the milleretids. In some parareptiles the ventral ramus is lacking (*Deltavjatia rossicus*, *Leptopleuron lacertinum*), tapers distally (*Mesosaurus tenuidens*), or is heavily grooved by the jugular canal (*Procolophon trigoniceps*). The pan-lepidosaurs generally display the plesiomorphic morphology. Transformation of this character to a club-shape is limited to stem-archosaurs. Recent efforts have distinguished several morphologies of the distal head of the ventral ramus in stem archosaurs (Spiekman et al., 2021), although we find that the variation noted by those authors likely warrants a breaking-up of their single, 4-state character into a pair of characters, respectively representing the distal part of the ramus and the proximal bridge of bone connecting the distal part to the main body of the element.

Prootic Contribution to Paroccipital Process—The prootic forms part of the anterior face of the paroccipital process across much of the reptilian tree. The few exceptions include the captorhinid *Labidosaurus hamatus*, the varanopid *Aerosaurus wellesi*, and crown turtles. The condition in *Proganochelys quenstedti* is not described. Based on our wider sample, the plesiomorphic condition for this character in Pan-Archosauria and, more broadly, Pan-Reptilia, is that the prootic contributes to the anterior face of the paroccipital process.

Semilunar Depression—The semilunar depression is a posterodorsally facing groove on the lateral face of the basitubera of the parabasisphenoid (Gower and Weber, 1998). This character was previously noted as present in all non-archosauriform pan-archosaurs (Nesbitt, 2011). However, we find that *Trilophosaurus*, *Macrocnemus*, and *Tanystropheus hydroides* do not bear this character (Spiekman et al., 2020). It is also absent outside of Pan-Archosauria after a review of several captorhinids, varanopids, parareptiles, and pan-lepidosaurs, although Pritchard et al. (2018) and Pritchard and Sues (2019) score the character as present in *Iguana iguana* and *Clevosaurus hudsoni*. This character is present in some early Pan-Archosaurs, but is absent from the crown (Gower, 1997), and no well-supported hypotheses of the function of the depression have been advanced at this time. Our reanalysis of the Pritchard and Sues (2019) matrix scoring the semilunar depression as absent in *Trilophosaurus* shows that this character is important in the structure of early Pan-Archosaur relationships and that some of those early relationships are not supported by many characters.

Fusion of the Exoccipital—Fusion of the exoccipital to other braincase elements, particularly the basioccipital and opisthotic, occurs across Pan-Reptilia. These characters have an enigmatic distribution that may be more indicative of ontogenetic than phylogenetic variation in fossil specimens, though some patterns are still apparent. The basioccipital and the exoccipital fuse in the early-diverging branches of Pan-Reptilia, though *Petrolacosaurus kansensis* and some parareptiles (*Procolophon trigoniceps*, *Leptopleuron lacertinum*, and *Belebey vegrandis*) have a distinct basioccipital and exoccipitals. The reptilian crown node is ambiguous, as pan-lepidosaurs show the unfused state, while early-diverging pan-archosaurs have exoccipitals variably fused to the basioccipital, with later transformation along that lineage to an unfused state. The earliest stem-turtle, *Eunotosaurus africanus* has no fusion of the exoccipitals to the basioccipital (Bever et al., 2015) and this condition is consistent with the crown, though no suture is visible between those elements in *Proganochelys quenstedti*.

Fusion of the exoccipital and the opisthotic to form the otoccipital is a more limited character state than exoccipital fusion to the basioccipital. The reptilian crown node is likely characterized by unfused exoccipitals and opisthotics, with a transition to the fused form taking place in the lepidosaur lineage crownward of *Placodus gigas*. In the pan-archosaurs, some early diverging taxa have a fused otoccipital (e.g., *Tanystropheus hydroides*, Spiekman et al., 2020), but the otoccipital is stably expressed in the crown (Jollie, 1957; Iordansky, 1974), with some transition to the stable expression between the reptilian and the archosaurian crown nodes. The exoccipital and opisthotic are fused in neither stem nor crown turtles. Fusion of the exoccipital to the opisthotic makes it difficult to score dorsal contralateral contact of the exoccipitals, though that condition is only noted in *Erythrosuchus africanus* and *Prolacerta broomi* of all the taxa that we reviewed, thus indicating a possible crownward transformation in the pan-archosaurs.

From this wider comparative context, it is apparent that an early pattern of exoccipital fusion to the basioccipital and a distinct opisthotic transitioned to a distinct basioccipital with fusion of the exoccipital to the opisthotic somewhere along both the archosaur and lepidosaur stem lineages. The variable condition we note in the three specimens of *Trilophosaurus* described here could represent a transitional state in which the developmental regulatory pathways leading towards fusion of the basioccipital to the exoccipitals are becoming less stably expressed, while the pathways leading to fusion of the exoccipitals to the opisthotics are being canalized. An alternative to this hypothesis is that these patterns found in the fossil record are reflections of ontogenetic rather than phylogenetic variation. Fusion of braincase elements is generally a late-stage ontogenetic event (Maisano, 2001, 2002), and thus some variability of these patterns should be expected, especially in a fossil record that is likely composed primarily of sub-adults (Erickson, 2005). A thorough analysis of the ontogenetic state of reptilian specimens using all available data should be part of any future descriptions (Griffin et al., 2021) to clarify the polarization of characters that may be prone to ontogenetic variation. A further complicating factor is that elements that appear fused on the surface may have a clear suture when the internal structure is examined via CT data. Given that many of the early taxa reviewed here were described in the absence of CT data, this could skew our understanding of the phylogenetic distribution of fusion-related characters. Proximally, we need closer study of the early-diverging stem-archosaurs to test hypotheses of transitional states in taxa such as *Trilophosaurus*. Many of the classic taxa across Pan-Reptilia also must be revisited using updated techniques (CT) in order to assist in polarization of morphological characters.

Exoccipital Contribution to the Basioccipital Condyle and Ventral Contact—The plesiomorphic condition of exoccipital fusion to the basioccipital presents problems for any characters attempting to distinguish ventral features of the exoccipitals. Thus, we found that among most early-diverging pan-reptilian taxa, the exoccipital contribution to the occipital condyle and contralateral contact of the exoccipitals ventral to the foramen magnum was unscorable. In taxa where the exoccipitals were not fused to the basioccipital, the exoccipitals contributed to the occipital condyle, and there was variable presence of ventral contralateral contact. The only taxa that diverge from this pattern are the stem lepidosaurs reviewed here, which all show no exoccipital contribution to the occipital condyle, though the contribution is present in the crown taxa. In none of the pan-lepidosaurs is there ventral contralateral contact of the exoccipitals. Although the phylogenetic signal of exoccipital contralateral contact below the foramen magnum is ambiguous, there is a clear signal that the exoccipitals contribute to the occipital condyle in the plesiomorphic condition for Pan-Reptilia.

Medial Ridge on the Dorsal Surface of the Basioccipital and Parabasisphenoid—In many pan-reptiles, a midline ridge on

the dorsal surface of the braincase floor conforms to the midline sulcus of the medulla oblongata and may represent a site of attachment for the bifid ligament of that part of the brain (Heaton, 1979; Evans, 1986). This ridge is present in all taxa we reviewed except *Petrolacosaurus kansensis*, the varanopids, the parareptiles *Deltavjatia rossicus* and *Mesosaurus tenuidens*, and *Erythrosuchus africanus.* The crown lepidosaurs also lack the feature. Though there are clearly some exceptions, this feature seems to be the plesiomorphic condition for pan-reptilia, with apomorphic loss among the varanopids, crown lepidosaurs, and some other select taxa.

Path of CN VI—Cranial nerve VI, the abducens nerve, leaves an osseus trace just posterior to the hypophyseal fossa in most pan-reptiles. The plesiomorphic condition is for CN VI to pierce the lateral parts of the dorsum sellae or the clinoid processes, as represented in the captorhinids, varanopids, many parareptiles, pan-lepidosaurs, and pan-turtles. There is some departure from this condition, particularly in *Procolophon trigoniceps*, *Youngina*, *Trilophosaurus*, and *Euparkeria*. These secondary departures from the plesiomorphic condition are likely autapomorphic, as is the entirely prootic-contained passage of *Erythrosuchus africanus.*

Neurocranial Pneumatization—The neurocranium of both crocodile- and bird-line crown archosaurs is highly pneumatized (Witmer and Ridgely, 2009; Dufeau and Witmer, 2015), supporting the phylogenetically justified conclusion that this character system was present in the ancestral crown archosaur and thus originated somewhere along the archosaurian stem lineage. Under this hypothesis, the earliest stem members of both Pan-Crocodylia and Pan-Aves would be pneumatized. This prediction has yet to be confirmed empirically, leaving open the possibility that braincase pneumaticity evolved multiple times within Pan-Archosauria—at least twice within the crown and perhaps along one or more stem lineages.

The phylogenetically earliest reported occurrence of pneumatization in a pan-archosaur is for the Triassic rhynchosaur, *Mesosuchus* (Sobral and Müller, 2019), whose relevant morphology is similar to that of *Trilophosaurus* in a number of ways. The neurocranial elements of both taxa exhibit an internal architecture characterized by a network of small, cell-like cavities that are well-delineated in cancellous bone and that are collectively surrounded by a thickened rind of superficial cortical bone. A thickened cortical region is also present in *Youngina* and turtles, and thus is likely plesiomorphic for Pan-Archosauria. Squamates exhibit what appears to be a derived form of endosteal expansion in these elements, with a reduced ratio of bone to open space. The network of small cell-like cavities does appear to be more extensive in *Trilophosaurus* and *Mesosuchus* than in either *Youngina* or turtles, suggesting a derived pan-archosaur condition. The difficulty of confidently assessing this variation qualitatively requires that a clear declaration of apomorphy be accompanied by expanded taxonomic sampling and quantitative analyses, which is outside the scope of this study. Even if a derived signal were established, it would remain unclear whether the expanded network of small, internal cells in these early pan-archosaurs was related to pneumatization. The question of pneumatization in the braincase of *Trilophosaurus* and *Mesosuchus* thus depends on how one interprets the larger internal cavities and their purported communications with the extracranial space – a diagnostic criterion for accepting pneumatization in fossils (Witmer, 1990).

The best evidence for pneumatization in *Trilophosaurus* is within the parabasisphenoid where an enlarged midline cavity is accompanied by a pair of bilaterally symmetrical openings into the underlying subcranial space. The cavity itself compares closely in size, shape, and extent between specimens, which supports their collective status as a morphologically 'real' feature and not an artifact of poor preservation. The external openings associated with this space, however, exhibit marked inter-specimen differences. In TMM 31025-244, the openings are elongate, vertically oriented fissures that communicate directly with the ventral surface of the parabasisphenoid, whereas in TMM 31100-443, the cavities open into a pair of bilaterally symmetrical, internal canals that extend a short distance ventromedially before converging as a single vertical canal. This relatively long canal penetrates the ventral surface of the parabasisphenoid as a circular foramen. The range of variation expands even further as we extend the comparisons to *Mesosuchus.* Here, the parabasisphenoid houses a pair of enlarged cavities that are centered more posteriorly than that of *Trilophosaurus*, invading the basitubera. Unlike in *Trilophosaurus*, the cavities open directly (no associated canal) into a poorly ossified region between the parabasisphenoid and basioccipital through openings that are only partially delimited in bone.

An additional space in the basioccipital of TMM 31100-443 with an associated foramen bears the signatures of a pneumatic origin. This internal cavity is smaller in extent than the cavity in the parabasisphenoid and is limited to the right side of the specimen. The strikingly regular foramen suggests that it is an anatomically 'real' opening, although the relatively thin bone in this area and the lack of a foramen on the contralateral side of TMM 31100-443 or in the other specimens warrants a degree of caution. The recess and foramen are positionally homologous to the subcondylar recess of Pan-Aves, a recess wherein the identity of the invading pneumatic system is unclear (Witmer and Ridgely, 2009). To our knowledge, no other stem-archosaurs exhibit evidence of a pneumatic cavity in this area; this may reflect the autapomorphic nature of the *Trilophosaurus* basioccipital plate, which entirely circumscribes the cavity in question.

Differences cannot themselves adjudicate questions of primary homology (sensu de Pinna, 1991). A basic tenet of comparative biology, often discussed under the moniker "Hennig's Auxiliary Principle" (see Wiley et al., 1991) sets the null hypothesis for any shared feature as homology, with the burden of proof falling squarely on the shoulders of any attempt to reject that homology null. Because differences may simply reflect the imposition of derived changes onto a homologous core (see Sereno, 2007), tree topology (i.e., secondary homology) is the only true arbiter of such questions (although see Wagner, 2014). It is also important to keep in mind that the initial stem signatures of a character system are likely to be subtler that the expression of that character system in the associated crown clade, and that a crown-based criterion for the character system's presence/absence might be overly demanding for the stem. Balancing this possibility with the concern for overinterpreting the data is one reason establishing evolutionary origins is so difficult.

Thus, the paired parabasisphenoid cavity of *Mesosuchus* may share primary homology with the midline cavity of *Trilophosaurus*, as may the different forms of openings that connect these cavities with the subcranial space. In the same respect, the basioccipital space may share primary homology with the subcondylar recess of Pan-Aves. The fundamental question here is whether these openings were present during life and not artifacts of preservation/decay, which would negate their relevance when considering the deep history of Pan-Archosaurian pneumatization. It cannot be denied that these particular differences between taxa give one pause. At the same time, the evidence is far from convincing that these openings can be dismissed as coincidental damage and/or that they clearly did not convey pneumatic diverticula. We thus tentatively accept the conclusions of Sobral and Müller (2019) that the neurocranium of at least some early pan-archosaurs was pneumatic. Most published hypotheses place the *Trilophosaurus* lineage as diverging from the main archosaur line prior to that of *Mesosuchus*, which means that *Trilophosaurus* represents the phylogenetically earliest expression of pan-archosaurian pneumatization.

The median pharyngeal recess is often associated with pneumatization in the pan-archosaurs. A shallow recess on the ventral surface of the parabasisphenoid similar to that in *Tanystropheus hyrdroides* (Spiekman et al., 2020) is found outside of the archosaur total group, including in the parareptiles *Deltavjatia rossicus* (Tsuji, 2013), *Leptopleuron lacertinum* (Spencer, 2000), and *Belebey vegrandis* (Reisz et al., 2007) and *Youngina capensis*. A larger recess is present on the ventral surface of the basisphenoid in the stem lepidosaur *Placodus gigas* (Neenan and Scheyer, 2012). Thus, the secondary homology of any ventral recess on the parabasisphenoid with the pneumatic median pharyngeal recess of crown archosaurs is unclear. The plesiomorphic condition for the group may resemble the condition in *Youngina capensis* and *Tanystropheus hydroides*, with excavation by pneumatic sinuses crownward of the tanystropheids resulting in a structure more similar to that found in *Trilophosaurus*.

With the above discussion and noted reservations in mind, we hypothesize that pan-archosaur neurocranial pneumatization began with the excavation of the median pharyngeal recess by a diverticulum of the pharyngeal pneumatic system. The presence of pneumatic cavities in both the basioccipital and basisphenoid in *Trilophosaurus* does not allow us to determine the sequence of invasions into the various neurocranial elements, although we might expect that a similar developmental process would underlie the invasion of any bone by a pneumatic system. As with any complex morphological character, a full understanding of the series of evolutionary transformations will only come with more dense taxonomic sampling. CT-based evidence for cranial pneumaticity also exists for the stem archosaurs *Eohyosaurus wolvaardti* and *Euparkeria capensis*, which like *Mesosuchus*, have paired internal cavities of the parabasisphenoid that invade the basitubera (Sobral and Müller, 2019), but no separate basioccipital cavities. Evidence for cranial pneumaticity among stem archosaurs lacking CT data (mainly in the form of foramina opening into the parabasisphenoid) was reviewed by Sobral and Müller (2019), and includes the rhynchosaurs *Howesia browni*, *Hyperodapedon gordoni*, and *Teyumbaita sulcognathus*, *Pamelaria dolichotrachela,* and *Erythrosuchus africanus*. The only taxon we would add to their treatment, besides *Trilophosaurus buettneri*, is *Azendohsaurus madagaskarensis*, for which Flynn et al. (2010) described foramen on the lateral surface of the basitubera. The invasion of the basipterygoid processes and basitubera by what became a paired internal pneumatic cavity, as evidenced by *Mesosuchus*, *Eohyosaurus*, and *Euparkeria* (Sobral and Müller, 2019), would (under this transformation model) represent a subsequent step in the evolution of this character system.

CT-based taxonomic sampling for pneumatic features among stem members of Pan-Archosauria is only just beginning, but the short current list of *Trilophosaurus*, *Mesosuchus*, *Eohyosaurus*, *Euparkeria*, and the taxa that bear parabasisphenoid foramina suggests convergence as a real possibility during this early history. Once a median pharyngeal recess housing a pneumatic sac was in place, it is not difficult to imagine such a configuration giving rise to multiple secondary invasions of the parabasisphenoid and thus a homoplastic pattern of basal-plate pneumatization across the pan-archosaur radiation. Further sampling will illuminate these possibilities. The seeming absence of pneumatic foramina on the posterior face of the basioccipital among stem archosaurs besides *Trilophosaurus* also supports a homoplastic distribution of subcondylar pneumaticity in the Pan-Archosaur radiation. The invasion of pneumatizing epithelium into the basioccipital may occur only with near-midline basioccipital 'material' available for occupation, as is the case with the broad basioccipital plate of *Trilophosaurus*. Based on the comparative principles referenced above, primary homology between the pneumatic features of these stem archosaurs and those of crown crocodilians and birds must also be considered the working hypothesis. Rejection of their secondary homology, however, would occur, if the earliest stem members of Pan-Crocodylia and Pan-Aves lacked the predicted signatures of braincase pneumatization.

If the above hypotheses withstand subsequent sampling and scrutiny, the neurocranium appears to be the first skeletal region of Pan-Archosauria to become pneumatized. The pneumatized antorbital cavity is a later, archosauriform addition to the pan-archosaur body plan (Witmer, 1997). Although external foramina were noted on the vertebrae of *Erythrosuchus africanus* (Gower, 2001), subsequent CT-based studies found no clear link between those foramina and internal cavities (Butler et al., 2012). Thus, postcranial pneumaticity may be restricted to Pan-Aves.

CONCLUSIONS

The first in-depth CT-based study of the *Trilophosaurus* braincase reveals a wealth of detail and insights that were beyond the reach of previous descriptive attempts. Such details help establish the ancestral conditions for a variety of pan-archosaurian features that are well studied in later forms, including the early transformations of the famously complex system of neurocranial pneumatization. These details also include autapomorphies, such as a derived inner ear geometry, that are congruent with previous proposals that *Trilophosaurus* was highly agile and capable of derived behaviors. Whether this included advanced forms of digging, climbing, running, or something else remains very much unsettled. Some clarity may come from a careful analysis of how the overall dimensions of the neurocranium and surrounding skull allow the transmission of high occlusal forces to the posterior part of the tooth row.

Perhaps more importantly, these derived morphologies contribute to an increasingly clear signal that pan-archosaurs achieved high levels of structural, behavioral, and ecological complexity early in their evolutionary history. Such early complexity is not necessarily surprising considering the diversity this radiation would ultimately produce; however, the effective absence of early forms that meet reasonable predictions of what an ancestral archosaur 'should' look like is notable as it suggests that progress on such problems as a clear morphological link between pan-turtles and pan-archosaurs (if one indeed exists) may require additional fossil discoveries. Still, it is undeniable that with each detailed descriptive study, our understanding of this deep history leaps forward and that consilience on a variety of issues in early reptilian evolution may be closer than we might think.

ACKNOWLEDGMENTS

We thank M. Colbert, J. Maisano, T. Rowe, M. Brown (UT Austin) for all their help in gaining access to these specimens and for procuring CT images. We thank D. Cerio, E. Huang, F. Torres, W. Foster, and A. Balanoff (JHU) for helpful comments and criticisms. We thank L. Ekl for assistance with figures and supplementary videos. We thank J. Merck for important insight regarding the overall dimensions of the braincase and its relation to occlusal forces. We also thank D. Dilkes, J. Merck, one anonymous reviewer, and the JVP editors for their helpful comments during the preparation of this study. This work was supported in part by NSF EAR 1943286 to SJN and NSF-DEB 1947025 to GSB.

ORCID

Sterling Nesbitt http://orcid.org/0000-0002-7017-1652

LITERATURE CITED

Bell, C. J., J. A. Gauthier, and G. S. Bever. 2010. Covert biases, circularity, and apomorphies: a critical look at the North American Quaternary

Herpetofaunal Stability Hypothesis. Quaternary International 217:30–36.
Bellairs, A. d'A., and A. M. Kamal. 1981. The chondrocranium and the development of the skull in recent reptiles; pp. 1–263 in C. Gans and T. S. Parsons (eds.), Biology of the Reptilia. Volume 11. Morphology F., 1st ed. Academic Press, London, New York, Toronto, Sydney, and San Francisco.
Benton, M. J. 1999. *Scleromochlus taylori* and the origin of dinosaurs and pterosaurs. Philosophical Transactions of the Royal Society B: Biological Sciences 354:1423–1446.
Bever, G. S. 2005. Variation in the ilium of North American *Bufo* (Lissamphibia; Anura) and its implications for species-level identification of fragmentary anuran fossils. Journal of Vertebrate Paleontology 25:548–560.
Bever, G. S. 2009a. The postnatal skull of the extant North American turtle *Pseudemys texana* (Cryptodira: Emydidae) with comments on the study of discrete intraspecific variation. Journal of Morphology 270:97–128.
Bever, G. S. 2009b. Postnatal ontogeny of the skull in the extant North American turtle *Sternotherus odoratus* (Cryptodira: Kinosternidae). Bulletin of the American Museum of Natural History 330:1–97.
Bever, G. S., C. J. Bell, and J. A. Maisano. 2005. The ossified braincase and cephalic osteoderms of *Shinisaurus crocodilurus* (Squamata, Shinisauridae). Palaeontologia Electronica 8:1–36.
Bever, G. S., T. R. Lyson, D. J. Field, and B. A. S. Bhullar. 2015. Evolutionary origin of the turtle skull. Nature 525:239–242.
Bhullar, B. A. S., and G. S. Bever. 2009. An archosaur-like laterosphenoid in early turtles (Reptilia: Pantestudines). Breviora 518:1–11.
Brown, E. E., R. J. Butler, M. D. Ezcurra, B. A. S. Bhullar, and S. Lautenschlager. 2019. Endocranial anatomy and life habits of the early triassic archosauriform *Proterosuchus fergusi*. Palaeontology 63:255–282.
Butler, R. J., P. M. Barrett, and D. J. Gower. 2012. Reassessment of the evidence for postcranial skeletal pneumaticity in Triassic archosaurs, and the early evolution of the avian respiratory system. PLOS One 7:e34094.
Campione, N. E., and R. R. Reisz. 2010. *Varanops brevirostris* (Eupelycosauria: Varanopidae) from the Lower Permian of Texas, with discussion of varanopid morphology and interrelationships. Journal of Vertebrate Paleontology 30:724–746.
Carroll, R. L. 1981. Plesiosaur ancestors from the Upper Permian of Madagascar. Philosophical Transactions of the Royal Society B: Biological Sciences 293:315–383.
Carroll, R. L., and W. Lindsay. 1985. Cranial anatomy of the primitive reptile *Procolophon*. Canadian Journal of Earth Sciences 22:1571–1587.
Case, E. C. 1928. A cotylosaur from the Upper Triassic of western Texas. Journal of the Washington Academy of Sciences 18:177–178.
Clark, J. M., J. Welman, J. A. Gauthier, and J. M. Parrish. 1993. The laterosphenoid bone of early archosauriforms. Journal of Vertebrate Paleontology 13:48–57.
Currey, J. D. 1999. The design of mineralised hard tissues for their mechanical functions. Journal of Experimental Biology 202:3285–3294.
Currie, P. J. 1997. Braincase anatomy; pp. 81–85 in K. Padian and P. Currie (eds.), Encyclopedia of Dinosaurs. Academic Press, San Diego, California.
David, R., M. Bronzati, and R. B. J. Benson. 2022. Comment on "The early origin of a birdlike inner ear and the evolution of dinosaurian movement and vocalization". Science 376:eabl6710.
deBraga, M., J. J. Bevitt, and R. R. Reisz. 2019. A new captorhinid from the Permian cave system near Richards Spur, Oklahoma, and the taxic diversity of *Captorhinus* at this locality. Frontiers in Earth Science 7:112.
de Pinna, M. C. C. 1991. Concepts and tests of homology in the cladistic paradigm. Cladistics 7: 367–394.
Dilkes, D. W. 1998. The early Triassic rhynchosaur *Mesosuchus browni* and the interrelationships of basal archosauromorph reptiles. Philosophical Transactions of the Royal Society B: Biological Sciences 353:501–541.
Donoghue, M. J., J. A. Doyle, J. Gauthier, A. G. Kluge, and T. Rowe. 1989. The importance of fossils in phylogeny reconstruction. Annual Review of Ecology and Systematics 20:431–460.
Dufeau, D. L., and L. M. Witmer. 2015. Ontogeny of the middle-ear air-sinus system in *Alligator mississippiensis* (Archosauria:Crocodylia). PLoS ONE 10:e0137060.
Dunay, R. E., and M. J. Fisher. 1979. Palynology of the Dockum Group (Upper Triassic), Texas, U.S.A. Review of Palaeobotany and Palynology 28:61–92.
Elder, R. L. 1987. Taphonomy and paleoecology of the Dockum Group, Howard County, Texas. Journal of the Arizona-Nevada Academy of Science 22:85–94.
Erickson, G. M. 2005. Assessing dinosaur growth patterns: a microscopic revolution. Trends in Ecology and Evolution 20:677–684.
Erwin, D. H. 2008. Extinction as the loss of evolutionary history. Proceedings of the National Academy of Sciences 105:11520–11527.
Evans, S. E. 1986. The braincase of *Prolacerta broomi* (Reptilia, Triassic). Neues Jahrbuch für Geologie und Paläontologie - Abhandlungen 173:181–200.
Evans, S. E. 1987. The braincase of *Youngina capensis* (Reptilia; Diapsida; Permian). Neues Jahrbuch für Geologie und Paläontologie - Monatshefte. 1987:193–203.
Evans, S. E. 2008. The Skull of Lizards and Tuatara; pp. 1–348 in C. Gans, A. S. Gaunt, and K. Adler (eds.), Biology of the Reptilia. Volume 20. Morphology H., 1st ed. Society for the Study of Amphibians and Reptiles, Ithaca.
Ezcurra, M. D. 2016. The phylogenetic relationships of basal archosauromorphs, with an emphasis on the systematics of proterosuchian archosauriforms. PeerJ 4:e1778.
Ezcurra, M. D., and R. J. Butler. 2018. The rise of the ruling reptiles and ecosystem recovery from the Permo-Triassic mass extinction. Proceedings of the Royal Society B: Biological Sciences 285:20180361.
Ezcurra, M. D., S. J. Nesbitt, M. Bronzati, F. M. Dalla Vecchia, F. L. Agnolin, R. B. J. Benson, F. Brissón Egli, S. F. Cabreira, S. W. Evers, A. R. Gentil, R. B. Irmis, A. G. Martinelli, F. E. Novas, L. Roberto da Silva, N. D. Smith, M. R. Stocker, A. H. Turner, and M. C. Langer. 2020. Enigmatic dinosaur precursors bridge the gap to the origin of Pterosauria. Nature 588:445–449.
Flynn, J. J., S. J. Nesbitt, J. M. Parrish, L. Ranivoharimanana, and A. R. Wyss. 2010. A new species of *Azendohsaurus* (Diapsida: Archosauromorpha) from the Triassic Isalo Group of southwestern Madagascar: cranium and mandible. Paleontology 53:669–688.
Fox, R. C., and M. C. Bowman. 1966. Osteology and relationships of *Captorhinus aguti* (Cope) (Reptilia: Captorhinomorpha). The University of Kansas Paleontological Contributions Vertebrata 11:1–79.
Gaffney, E. S. 1979. Comparative cranial morphology of recent and fossil turtles. Bulletin of the American Museum of Natural History 164:67–376.
Gaffney, E. S. 1990. The comparative osteology of the Triassic turtle *Proganochelys*. Bulletin of the American Museum of Natural History. 194:1–263.
Gans, C., and R. Montero. 2008. An atlas of amphisbaenian skull anatomy; pp. 621–738 in C. Gans and R. Montero (eds.), Biology of the Reptilia. Volume 21. Morphology I. The Skull and Appendicular Locomotor Apparatus of Lepidosauria. Society for the Study of Amphibians and Reptiles, Ithaca.
Gardner, N. M., C. M. Holliday, and F. R. O'Keefe. 2010. The braincase of *Youngina capensis* (Reptilia, Diapsida): new insights from high-resolution CT scanning of the holotype. Palaeontologia Electronica 13:19A.
Gauthier, J. A. 1986. Saurischian monophyly and the origin of birds. Memoirs of the California Academy of Sciences 8:1–55.
Gauthier, J. A., M. Kearney, J. A. Maisano, O. Rieppel, and A. D. B. Behlke. 2012. Assembling the squamate tree of life: perspectives from the phenotype and the fossil record. Bulletin of the Peabody Museum of Natural History 53:3–308.
Georgi, J. A., J. S. Sipla, and C. A. Forster. 2013. Turning semicircular canal function on its head: dinosaurs and a novel vestibular analysis. PLoS ONE 8:e58517.
Gottmann-Quesada, A., and P. M. Sander. 2009. A redescription of the early archosauromorph *Protorosaurus speneri* Meyer, 1832, and its phylogenetic relationships. Palaeontographica Abteilung A 287: 123–220.
Gow, C. E. 1972. The osteology and relationships of the Millerettidae (Reptilia: Cotylosauria). Journal of Zoology 167:219–264.
Gow, C. E. 1975. The morphology and relationships of *Youngina capensis* Broom and *Prolacerta broomi* Parrington. Palaeontologica Africana 18:89–131.

Gower, D. J. 1997. The braincase of the early archosaurian reptile *Erythrosuchus africanus*. Journal of Zoology 242:557–576.
Gower, D. J. 2001. Possible postcranial pneumaticity in the last common ancestor of birds and crocodilians: evidence from *Erythrosuchus* and other Mesozoic archosaurs. Naturwissenschaften 88:119–122.
Gower, D. J., and A. G. Sennikov. 1996. Morphology and phylogenetic informativeness of early archosaur braincases. Palaeontology 39:883–906.
Gower, D. J., and E. Weber. 1998. The braincase of *Euparkeria*, and the evolutionary relationships of birds and crocodilians. Biological Reviews 73:367–411.
Gregory, J. T. 1945. Osteology and relationships of *Trilophosaurus*. University of Texas Publications 4401:273–359.
Griffin, C. T., M. R. Stocker, C. Colleary, C. M. Stefanic, E. J. Lessner, M. Riegler, K. Formoso, K. Koeller, and S. J. Nesbitt. 2021. Assessing ontogenetic maturity in extinct saurian reptiles. Biological Reviews 96:470–525.
Hanson, M., E. A. Hoffman, M. A. Norell, and B. A. S. Bhullar. 2021. The early origin of a birdlike inner ear and the evolution of dinosaurian movement and vocalization. Science 372:601–609.
Hanson, M., E. A. Hoffman, M. A. Norell, and B. A. S. Bhullar. 2022. Response to comment on "The early origin of a birdlike inner ear and the evolution of dinosaurian movement and vocalization". 376:eabl8181.
Heaton, M. J. 1979. Cranial anatomy of primitive captorhinid reptiles from the Late Pennsylvanian and Early Permian Oklahoma and Texas. Oklahoma Geological Survey 127:1–84.
Heckert, A. B., S. G. Lucas, L. F. Rinehart, J. A. Spielmann, A. P. Hunt, and R. Kahle. 2006. Revision of the archosauromorph reptile *Trilophosaurus*, with a description of the first skull of *Trilophosaurus jacobsi*, from the Upper Triassic Chinle Group, west Texas, USA. Palaeontology 49:621–640.
Hedges, S. B., J. Marin, M. Suleski, M. Paymer, and S. Kumar. 2015. Tree of life reveals clock-like speciation and diversification. Molecular Biology and Evolution 32:835–845.
Hone, D. W. E., A. A. Farke, and M. J. Wedel. 2016. Ontogeny and the fossil record: what, if anything, is an adult dinosaur? Biology Letters 12:20150947.
Hunt, A. P., and S. G. Lucas. 1991. The *Paleorhinus* biochron and the correlation of the non-marine Upper Triassic of Pangaea. Palaeontology 34:487–501.
Iordansky, N. N. 1974. The Skull of the Crocodilia; pp. 201–262 in C. Gans and T. S. Parsons (eds.), Biology of the Reptilia. Volume 4. Morphology D., 1st ed. Academic Press, London, New York, Toronto, Sydney, and San Francisco.
Jenkins, X, A., A. C. Pritchard, A. D. Marsh, B. T. Kligman, C. A. Sidor, and K. E. Reed. 2020. Using manual ungual morphology to predict substrate use in the Drepanosauromorpha and the description of a new species. Journal of Vertebrate Paleontology 40: e1810058.
Jollie, M. T. 1957. The head skeleton of the chicken and remarks on the anatomy of this region in other birds. Journal of Morphology 100:389–436.
Langston, W., and R. R. Reisz. 1981. *Aerosaurus wellesi*, new species, a varanopseid mammal-like reptile (Synapsida:Pelycosauria) from the Lower Permian of New Mexico. Journal of Vertebrate Paleontology 1:73–96.
Lauder, G. V. 1995. On the inference of function from structure; pp. 1–18 in J. J. Thomason (ed.), Functional Morphology in Vertebrate Paleontology, 1st ed. Cambridge University Press, Cambridge.
Lautenschlager, S., and R. J. Butler. 2016. Neural and endocranial anatomy of Triassic phytosaurian reptiles and convergence with fossil and modern crocodylians. PeerJ 4:e2251.
Li, C., X.-C. Wu, O. Rieppel, L.-T. Wang, and L.-J. Zhao. 2008. An ancestral turtle from the Late Triassic of southwestern China. Nature 456:497–501.
Li, C., N. C. Fraser, O. Rieppel, and X.-C. Wu. 2018. A Triassic stem turtle with an edentulous beak. Nature 560:476–479.
Maisano, J. A. 2001. A survey of state of ossification in neonatal squamates. Herpetological Monographs 15:135–157.
Maisano, J. A. 2002. Terminal fusions of skeletal elements as indicators of maturity in squamates. Journal of Vertebrate Paleontology 22:268–275.
Merck, J. W. 1995. The cranial anatomy of *Trilophosaurus buettneri* as revealed by high-resolution computer aided tomography. 55th Annual Meeting of the Society of Vertebrate Paleontology, Abstracts and Program, Pittsburgh, Pennsylvania.
Merck, J. W. 1997. A phylogenetic analysis of the euryapsid reptiles. Ph.D. dissertation, University of Texas at Austin, 785 pp.
Miedema, F., S. N. F. Spiekman, V. Fernandez, J. W. F. Reumer, and T. M. Scheyer. 2020. Cranial morphology of the tanystropheid *Macrocnemus bassanii* unveiled using synchrotron microtomography. Scientific Reports 10:12412.
Modesto, S. P. 2006. The cranial skeleton of the Early Permian aquatic reptile *Mesosaurus tenuidens*: implications for relationships and palaeobiology. Zoological Journal of the Linnean Society 146:345–368.
Modesto, S. P., D. M. Scott, D. S. Berman, J. Müller, and R. Reisz. 2007. The skull and the palaeoecological significance of *Labidosaurus hamatus*, a captorhinid reptile from the Lower Permian of Texas. Zoological Journal of the Linnean Society 149:237–262.
Montero, R., J. D. Daza, A. M. Bauer, and V. Abdala. 2017. How common are cranial sesamoids among squamates? Journal of Morphology 278:1400–1411.
Neenan, J. M., and T. M. Scheyer. 2012. The braincase and inner ear of *Placodus gigas* (Sauropterygia, Placodontia)—a new reconstruction based on micro-computed tomographic data. Journal of Vertebrate Paleontology 32:1350–1357.
Nesbitt, S. J. 2011. The early evolution of archosaurs: relationships and the origin of major clades. Bulletin of the American Museum of Natural History 352:1–292.
Nesbitt, S. J., and M. R. Stocker. 2008. Vertebrate assemblage of the Late Triassic Canjilon Quarry (northern New Mexico, USA), and the importance of apomorphy-based assemblage comparisons. Journal of Vertebrate Paleontology 28:1063–1072.
Nesbitt, S. J., J. J. Flynn, A. C. Pritchard, J. M. Parrish, L. Ranivoharimanana, and A. R. Wyss. 2015. Postcranial osteology of *Azendohsaurus madagaskarensis* (?Middle to Upper Triassic, Isalo Group, Madagascar) and its systematic position among stem archosaur reptiles. Bulletin of the American Museum of Natural History 398:1–126.
Nesbitt, S. J., M. R. Stocker, M. D. Ezcurra, N. C. Fraser, A. B. Heckert, W. G. Parker, B. Mueller, S. Sengupta, S. Bandyopadhyay, A. C. Pritchard, and A. D. Marsh. 2021. Widespread azendohsaurids (Archosauromorpha, Allokotosauria) from the Late Triassic of western USA and India. Papers in Paleontology 8:e1413.
O'Donoghue, C. H. 1920. The blood vascular system of the tuatara, *Sphenodon punctatus*. Philosophical Transactions of the Royal Society B: Biological Sciences 210:175–252.
Oelrich, T. M. 1956. The anatomy of the head of *Ctenosaura pectinata* (Iguanidae). Miscellaneous Publications, Museum of Zoology, University of Michigan 94:1–122.
Organ, C. L. 2006. Biomechanics of ossified tendons in ornithopod dinosaurs. Paleobiology 32:652–665.
Parker, W. G. 2013. Redescription and taxonomic status of specimens of *Episcoposaurus* and *Typothorax*, the earliest known aetosaurs (Archosauria: Suchia) from the Upper Triassic of western North America, and the problem of proxy "holotypes". Earth and Environmental Science Transactions of the Royal Society of Edinburgh 103:313–338.
Parks, P. 1969. Cranial Anatomy and Mastication of the Triassic Reptile *Trilophosaurus*. M.S. thesis, University of Texas at Austin, 88 pp.
Parrish, J. M. 1993. Phylogeny of the Crocodylotarsi, with reference to archosaurian and crurotarsan monophyly. Journal of Vertebrate Paleontology 13:287–308.
Patterson, C., and D. E. Rosen. 1977. Review of ichthyodectiform and other Mesozoic teleost fishes, and the history and practice of classifying fossils. Bulletin of the American Museum of Natural History 158:1–172.
Porter, W. R., and L. M. Witmer. 2015. Vascular patterns in iguanas and other squamates: blood vessels and sites of thermal exchange. PLOS One 10:e139215.
Pritchard, A. C., and H.-D. Sues. 2019. Postcranial remains of *Teraterpeton hrynewichorum* (Reptilia: Archosauromorpha) and the mosaic evolution of the saurian postcranial skeleton. Journal of Systematic Palaeontology 17:1745–1765.

Pritchard, A. C., J. A. Gauthier, M. Hanson, G. S. Bever, and B.-A. S. Bhullar. 2018. A tiny Triassic saurian from Connecticut and the early evolution of the diapsid feeding apparatus. Nature Communications 9:1213.

Pritchard, A. C., A. H. Turner, S. J. Nesbitt, R. B. Irmis, and N. D. Smith. 2015. Late Triassic tanystropheids (Reptilia, Archosauromorpha) from northern New Mexico (Petrified Forest Member, Chinle Formation) and the biogeography, functional morphology, and evolution of Tanystropheidae. Journal of Vertebrate Paleontology 35: e911186.

Price, L. I. 1935. Notes on the brain case of *Captorhinus*. Proceedings of the Boston Society of Natural History 40:377–386.

Reisz, R. R. 1981. A diapsid reptile from the Pennsylvanian of Kansas. Special Publication of the Museum of Natural History, University of Kansas 7:1–74.

Reisz, R. R., J. Müller, L. Tsuji, and D. Scott. 2007. The cranial osteology of *Belebey vegrandis* (Parareptilia: Bolosauridae), from the Middle Permian of Russia, and its bearing on reptilian evolution. Zoological Journal of the Linnean Society 151:191–214.

Rieppel, O. 1994. The braincases of *Simosaurus* and *Nothosaurus*: monophyly of the Nothosauridae (Reptilia: Sauropterygia). Journal of Vertebate Paleontology 14:9–23.

Sato, T., X.-C. Wu, A. Tirabasso, and P. Bloskie. 2011. Braincase of a polycotylid plesiosaur (Reptilia: Sauropterygia) from the Upper Cretaceous of Manitoba, Canada. Journal of Vertebrate Paleontology 31:313–329.

Scheyer, T. M., S. N. F. Spiekman, H.-D. Sues, M. D. Ezcurra, R. J. Butler, and M. E. H. Jones. 2020. *Colobops*: a juvenile rhynchocephalian reptile (Lepidosauromorpha), not a diminutive archosauromorph with an unusually strong bite. Royal Society Open Science 7:192179.

Schoch, R. R., and H.-D. Sues. 2018. Osteology of the Middle Triassic stem-turtle *Pappochelys rosinae* and the early evolution of the turtle skeleton. Journal of Vertebrate Paleontology 16:927–965.

Sereno, P. C. 2007. Logical basis for morphological characters in phylogenetics. Cladistics 23:565–587.

Simões, T. R., M. W. Caldwell, M. Tałanda, M. Bernardi, A. Palci, O. Vernygora, F. Bernardini, L. Mancini, and R. L. Nydam. 2018. The origin of squamates revealed by a Middle Triassic lizard from the Italian Alps. Nature 557:706–709.

Small, B. J. 2002. Cranial anatomy of *Desmatosuchus haplocerus* (Reptilia: Archosauria: Stagonolepidae). Zoological Journal of the Linnean Society 136:97–111.

Snively, E., and A. P. Russel. 2007. Functional morphology of neck musculature in the Tyrannosauridae (Dinosauria, Theropoda) as determined via a hierarchical inferential approach. Zoological Journal of the Linnean Society 151:759–808.

Sobral, G., and J. Müller. 2019. The braincase of *Mesosuchus browni* (Reptilia, Archosauromorpha) with information on the inner ear and description of a pneumatic sinus. PeerJ 7:e6798.

Sobral, G., R. B. Sookias, B. A. S. Bhullar, R. Smith, R. J. Butler, and J. Müller. 2016. New information on the braincase and inner ear of *Euparkeria capensis* Broom: implications for diapsid and archosaur evolution. Royal Society Open Science 3:160072.

Spencer, P. S. 2000. The braincase structure of *Leptopleuron lacertinum* Owen (Parareptilia: Procolophonidae). Journal of Vertebrate Paleontology 20:21–30.

Spiekman, S. N. F., N. C. Fraser, and T. M. Scheyer. 2021. A new phylogenetic hypothesis of Tanystropheidae (Diapsida, Archosauromorpha) and other "protorosaurs", and its implications for the early evolution of stem archosaurs. PeerJ 9:e11143.

Spiekman, S. N. F., J. M. Neenan, N. C. Fraser, V. Fernandez, O. Rieppel, S. Nosotti, and T. M. Scheyer. 2020. The cranial morphology of *Tanystropheus hydroides* (Tanystropheidae, Archosauromorpha) as revealed by synchrotron microtomography. PeerJ 8:e10299.

Spielmann, J. A., A. B. Heckert, and S. G. Lucas. 2005. The Late Triassic archosauromorph *Trilophosaurus* as an arboreal climber. Rivista Italiana Di Paleontologia e Stratigrafia 111:395–412.

Spielmann, J. A., S. G. Lucas, L. F. Rinehart, and A. B. Heckert. 2008. The Late Triassic archosauromorph *Trilophosaurus*. New Mexico Museum of Natural History and Science Bulletin 43:1–177.

Spoor, F., T. Garland, G. Krovitz, T. M. Ryan, M. T. Silcox, and A. Walker. 2007. The primate semicircular canal system and locomotion. Proceedings of the National Academy of Sciences 104:10808–10812.

Stocker, M. R. 2013. Contextualizing vertebrate faunal dynamics: new perspectives from the Triassic and Eocene of western North America. Ph.D. dissertation, the University of Texas at Austin, 297 pp.; Austin.

Stocker, M. R., S. J. Nesbitt, K. E. Criswell, W. G. Parker, L. M. Witmer, T. B. Rowe, R. Ridgely, and M. A. Brown. 2016. A dome-headed stem archosaur exemplifies convergence among dinosaurs and their distant relatives. Current Biology 26:2674–2680.

Töpfer, T. 2018. Morphological variation in birds: plasticity, adaptation, and speciation; pp. 63–74 in D. T. Tietze (ed.), Bird Species, 1st ed. Springer International Publishing, Cham.

Tsuihiji, T. 2007. Homologies of the *longissimus*, *iliocostalis*, and hypaxial muscles in the anterior presacral region of extant Diapsida. Journal of Morphology 268:986–1020.

Tsuji, L. A. 2013. Anatomy, cranial ontogeny and phylogenetic relationships of the pareiasaur *Deltavjatia rossicus* from the Late Permian of central Russia Earth and Environmental Science Transactions of the Royal Society of Edinburgh 104:81–122.

Vargas, A. O., M. Ruiz-Flores, S. Soto-Acuña, N. Haidr, C. Acosta-Hospitaleche, L. Ossa-Fuentes, and V. Muñoz-Walther. 2017. The origin and evolutionary consequences of skeletal traits shaped by embryonic muscular activity, from basal theropods to modern birds. Integrative and Comparative Biology 57:1281–1292.

Wagner, G. P. 2014. Homology, Genes, and Evolutionary Innovation. Princeton University Press, Princeton, NJ. 479 pp.

Walker, A. D. 1972. New light on the origin of birds and crocodiles. Nature 237:257–263.

Walker, A. D. 1990. A revision of *Sphenosuchus acutus* Haughton, a crocodylomorph reptile from the Elliot Formation (Late Triassic or Early Jurassic) of South Africa. Philosophical Transactions of the Royal Society B: Biological Sciences 330:1–120.

Wiley, E. O., D. Siegel-Causey, D. R. Brooks, and V. A. Funk. 1991. The Compleat Cladist: A Primer of Phylogenetic Procedures. University of Kansas Museum of Natural History, Special Publication 19. 158 pp.

Witmer, L. M. 1990. The craniofacial air sac system of Mesozoic birds (Aves). Zoological Journal of the Linnean Society 100:327–378.

Witmer, L. M. 1997. The evolution of the antorbital cavity of archosaurs: a study in soft-tissue reconstruction in the fossil record with an analysis of the function of pneumaticity. Journal of Vertebrate Paleontology 17:1–76.

Witmer, L. M., and R. C. Ridgely. 2009. New insights into the brain, braincase and ear region of tyrannosaurs (Dinosauria, Theropoda), with implications for sensory organization and behavior. Anatomical Record 292:1266–1296.

Zangerl, R. 1944. Contributions to the osteology of the skull of the Amphisbaenidae. The American Midland Naturalist 31:417–454.

Zhou, X., R. V. Pêgas, W. Ma, G. Han, X. Jin, M. E. C. Leal, N. Bonde, Y. Kobayashi, S. Lautenschlager, X. Wei, C. Shen, and S. Ji. 2021. A new darwinopteran pterosaur reveals arborealism and an opposed thumb. Current Biology 31:1–8.

Submitted May 18, 2022; revisions received August 15, 2022;
accepted August 25, 2022.
Handling Editor: Hans-Dieter Sues.